A NOVEL REGULATORY FUNCTION FOR P130 IN ADIPOCYTE FATTY ACID METABOLISM

NAREH RINEI EDJIU

A THESIS SUBMITTED TO
THE FACULTY OF GRADUATE STUDIES
IN PARTIAL FULFILLMENT OF THE REQUIREMTS
FOR THE DEGREE OF
MASTERS OF SCIENCE

GRADUATE PROGRAM IN KINESIOLOGY AND HEALTH SCIENCE
YORK UNIVERISTY
TORONTO, ONTARIO

SEPTEMBER 2017

ABSTRACT

Understanding the complex control mechanisms governing fatty acid synthesis and mobilization holds prognostic and therapeutic potential in treating metabolic diseases such as obesity and diabetes. Our data has uncovered a novel function for the transcriptional co-repressor p130 in adipocytes. In particular, we found that the subcellular localization of p130 supports fatty acid metabolism. Indeed, stimulating lipogenesis increased p130 levels in the mitochondria. Here it interacted at the D-loop regulatory region of mitochondrial DNA, repressing genes involved in oxidative phosphorylation. This could allow the intermediates of the TCA cycle to be utilized for lipid synthesis in lieu of energy production. Conversely, inducing lipolysis via β_3-adrenergic activation in white adipocytes or a physiological challenge imposed by fasting, decreased p130 levels in the mitochondria, concomitant with increased mitochondrial-encoded gene expression. Unexpectedly, β_3-adrenergic stimulation showed the reverse effect in brown adipocytes. Our results provide valuable insight for deconstructing the intricate metabolic framework of adipocytes.

Special Acknowledgements

I would first like to thank my supervisor, Dr. Anthony Scimè, for his relentless support and encouragement. You were right – I definitely grew "thick skin" over the course of my degree. Thank you for all your invaluable help and mentorship. Your words of reassurance will always resonate with me as I continue to pursue my career in science.

I would like to thank my senior lab members, Debasmita and Maryam, for their unwavering patience and guidance in teaching me the technical and analytical skills that are required to be a successful scientific researcher. I would also like to thank my lab mate, Ninoschka, for your great company during our late nights at the lab and for being not just a great colleague, but a better friend.

Thank you to my committee members, Dr. Michael Riddell and Dr. Michael Scheid, for always being willing to help and for their constant reassurance that I was on the right track.

Finally, I would like to thank my loving family, boyfriend, and friends for always showing a keen interest in my research and for helping me overcome any obstacles that I faced. You encouraged me not to give up and continue working hard.

TABLE OF CONTENTS

LIST OF TABLES

LIST OF FIGURES

Literature Review:

Results section:

LIST OF ABBREVIATIONS

ACC	Acetyl-CoA carboxylase
ACL	ATP citrate lyase
ATGL	Adipose triglyceride lipase
ATP	Adenosine triphosphate
ANOVA	Analysis of Variance
Atp6	ATP synthase Fo subunit 6 (Complex 5)
βAR	β-adrenergic receptors
BAT	Brown adipose tissue
BSA	Bovine serum albumin
cAMP/PKA	Cyclic AMP/ cAMP-dependent protein kinase
cDNA	Complementary DNA
ChIP	Chromatin Immunoprecipitation
CL	CL 316,243 (β_3-adrenergic agonist)
Cox2	Cytochrome c oxidase subunit 2 (Complex 4)
Cyt b	Cytochrome b (Complex 3)
DAG	Diacylglycerol
D-loop	Displacement loop
DMSO	Dimethyl sulfoxide
DMEM	Dulbecco's modified eagle medium
DTT	Dithiothreitol
EDTA	Ethylenediaminetetraacetic acid
ETC	Electron transport chain
FBS	Fetal bovine serum
$FADH_2$	Flavin adenine dinucleotide (reduced)
FAS	Fatty acid synthase
FA(s)	Fatty acid(s)
FTO	Fat mass and obesity associated gene locus
GWAS	genome-wide association studies
HEPES	N-2-hydroxyethylpiperazine-N-2-ethane sulfonic acid
HSL	Hormone sensitive lipase
HSP1/2	Heavy strand promoter 1/2
KD	Knockdown
KO	Knock out
LSD1	Lysine-specific demethylase 1
LSP	Light strand promoter
µL	Microlitres
MAG	Monoacylglycerol
MAPK	Mitogen-activated protein kinase
min	Minutes
MIQE	Minimum Information for Publication of Quantitative Real-Time PCR Experiments
mtDNA	Mitochondrial deoxyribonucleic acid
mTORC1	Aammalian target of rapamycin complex 1
NADH	Nicotinamide adenine dinucleotide (reduced)

NADPH	Nicotinamide adenine dinucleotide phosphate (reduced)
Nd4	NADH-ubiquinone oxidoreductase chain 4 (Complex 1)
OXPHOS	Oxidative Phosphorylation
PBS	Phosphate buffered saline
Pgc-1α	Pparγ coactivator 1 alpha
PI3K/Akt	Phosphatidylinositol-3-kinase/ Protein Kinase B
qChIP	Quantitative chromatin immunoprecipitation assay
qPCR	Quantitative polymerase chain reaction
Rb	Retinoblastoma susceptibility gene
RIPA	Radioimmunoprecipitation assay buffer
RNAi	Ribonucleic acid interference
ROS	Reactive oxygen species
rRNA	Ribosomal ribonucleic acid
RT	Room temperature
rpm	Rotations per minute
SCD1	Stearoyl-CoA desaturase
SD	Standard deviation
sh	Short hair pin
SDS	Sodium dodecyl sulfate
SNP	Single nucleotide polymorphisms
SREBP-1	Sterol regulatory element binding protein-1
SVF	Stromal vascular fraction
TAG	Triglyceride
T_3	Triiodothyronine
TBS	Tris-buffered saline
TCA	Tricarboxylic acid cycle
TFAm	Mitochondrial transcription factor A
Tris HCL	Trisaminomethane hydrochloride
tRNA	Transfer ribonucleic acid
Ucp-1	Uncoupling protein 1
WAT	White adipose tissue

1. LITERATURE REVIEW

White, brown and beige adipocytes

Rodents and humans possess different types of fat tissue, each with distinct physiological functions (Chen et al., 2016). White adipocytes located in white adipose tissue (WAT) depots function in triglyceride storage and act as important endocrine cells secreting hormones such as leptin and adiponectin (Costa and Duarte, 2006; Matsuzawa, 2006) (**Fig. 1**). Contrarily, brown and beige adipocytes dissipate energy through heat production in a process known as non-shivering thermogenesis. Beige adipocytes differ from brown adipocytes as they are inducible "brown-like" cells that develop in WAT in response to cold exposure or adrenergic stimulation (Harms and Seale, 2013; Wu et al., 2012). Despite their mutual involvement in non-shivering thermogenesis, beige and brown adipocytes originate from distinct developmental progenitors and possesses unique gene expression profiles (Porras et al., 2017; Harms and Seale, 2013; Gesta et al., 2007; Vitali et al., 2012; Peirce et al., 2014; Lazar, 2008; Wu et al., 2012; Algire et al., 2013). Thus, it is clear that white and thermogenic adipocytes have opposing roles in energy storage and consumption respectively (Rosell et al., 2014).

White adipocytes are found in three main anatomical regions in the human body that include the intra-abdominal (visceral), upper-body/abdominal (subcutaneous) and lower body subcutaneous adipose tissues (Tchkonia et al., 2013). In rodents, white adipocytes are largely found in the inguinal and epididymal fat pads (Chusyd et al., 2016). In adult humans, active brown and/or beige depots have been detected in the cervical, supraclavicular, axillary, and paravertebral regions assumed to have evolved for warming the blood supplying the brain (Sidossis and Kajimura, 2015). In human infants, brown

adipocytes are found in the interscapular and perirenal regions, and appear to remain present throughout adulthood but drastically reducing at a very early age (Lecoultre and Rayussin, 2011). In rodents, brown adipocytes are found in interscapular and perirenal BAT depots, while beige adipocytes are found interspersed within WAT depots (Sidossis and Kajimura, 2015).

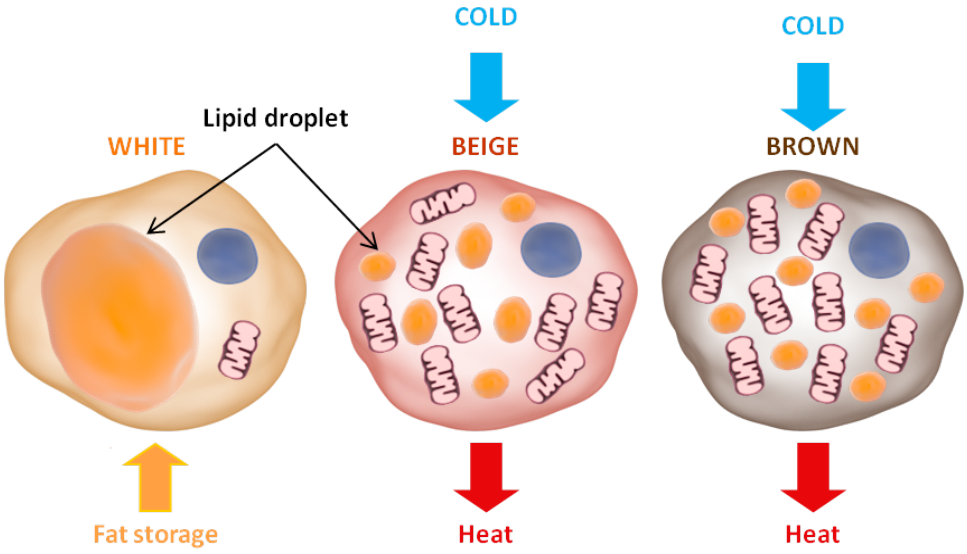

Figure 1. Features and functions of white, brown and beige adipocytes. White adipocytes function mainly in storing excess energy as triglycerides, whereas beige and brown adipocytes dissipate energy through heat production known as non-shivering thermogenesis. Brown and beige adipocytes have a relatively high mitochondrial content compared to white. They also contain many multilocular/small lipid droplets whereas white adipocytes have one lipid (unilocular) morphology.

Oxidative metabolism in adipocytes

Metabolic modulations regulating energy production govern whether a cell proliferates, differentiates or exits the cell cycle and enters a state of quiescence (Shyh-Chang et al., 2013). Furthermore, some metabolic pathways play an important role in dictating tissue lineage fates (Porras et al., 2017; van der Knapp and Verrijzer, 2016). In contrast to differentiated cells, proliferating stem/progenitor cells rely mainly on non-oxidative energy generation by glycolysis whereby the end product pyruvate is not used by

the mitochondria (Rafalski et al., 2012; Zhang et al., 2011; Zhou et al., 2012). Although glycolysis alone is less efficient in producing energy than the mitochondria that houses the tricarboxylic acid (TCA) cycle and the electron transport chain (ETC), it produces ATP at a faster rate with reduced generation of reactive oxygen species. In addition, glycolysis provides the necessary cofactors and metabolic intermediates to support the proliferative capacity of the cells (Folmes et al., 2012).

Differentiated cells require larger amounts of energy are required to sustain specialized functions. The decreased demand for anabolic substrates allows for increased energy conversion into ATP via oxidative phosphorylation (OXPHOS) that occurs in the mitochondria (Rafalski et al., 2012). In this case, pyruvate produced from glycolysis is converted into acetyl-CoA which enters the TCA cycle, also known as the Krebs cycle. The TCA cycle consists of a series of enzymatic reactions that oxidizes acetyl-CoA to produce energy and reducing equivalents (NADH and $FADH_2$), that are subsequently used as electron donors for the ETC (Sancho et al., 2016; Chandel, 2014). Several other carbon sources including pyruvate, glutamine and fatty acids can also feed into the TCA cycle to generate reducing equivalents. In the ETC as electrons are passed from the reducing agents along the protein complexes, an electrochemical gradient is established which helps to drive ATP synthesis in the final step of the ETC (Chandel, 2014).

The metabolic switch from glycolytic to oxidative energy metabolism begins early during adipogenic stem cell differentiation. This energetic shift is fundamental in supporting the biological function and survival of differentiated adipocytes that preferentially rely on OXPHOS to synthesize larger amounts of ATP (Drehmer et al., 2016). Several studies investigating the adipocyte progenitor cell line 3T3-L1

differentiation into white adipocytes have revealed an activation of mitochondrial biogenesis during the process, representing the importance of increased mitochondrial mass in supporting the metabolic nature and function of differentiated white adipocytes (Wilson-Fritch, L, et al., 2003).

Role of mitochondria in adipocytes

In terminally differentiated adipocytes, energy metabolism is central to supporting their specialized functions. For this, mitochondria are highly dynamic organelles that play a major role in processes such as lipogenesis and lipolysis, the production of ROS and OXPHOS (Cedikova et al., 2016). In addition, mitochondria are essential for proper differentiation of adipocyte progenitors and contribute to the adipocyte production and secretion of adipokines, such as leptin (De Pauw et al., 2009; Koh et al., 2007).

All living organisms depend on an efficient energy generating system for cell survival and proper functioning. Mitochondria are key players involved in fuelling several cellular processes and can be characterized as labile energy factories that respond to the metabolic demands of the cell. Mitochondria are critical players in adipose metabolism, as prominent mitochondrial defects are commonly present in several metabolic diseases (Crunkhorn and Patti, 2008; Holloway et al., 2009 ; Turner and Heilbronn, 2008). Differences of mouse mitochondrial protein expression within adipocyte lineages are related to the specialized metabolic functions of white and brown fat (Forner et al., 2009). In vivo comparisons of the two mitochondrial proteomes uncovered quantitative and qualitative distinctions, which can directly relate to the unique metabolic activities in these fat types. Catabolic processes including fatty acid (FA) metabolism, TCA cycle and

OXPHOS were predominant mitochondrial activities in brown fat, suggested by the relative enrichment of proteins involved in these metabolic pathways. Conversely in white adipocytes, mitochondria were characterized by anabolic functions such as glycerolipid and triglyceride biosynthesis via lipogenic routes involving the TCA cycle (Forner et al., 2009). This was indicated by the augmentation of proteins involved in de novo lipogenesis among which included pyruvate carboxylase which converts pyruvate into oxaloacetate that can be subsequently converted into citrate. Citrate is able to cross inner mitochondrial membrane into the cytosol where it participates in FA biosynthesis (Mounier et al., 2014; Ferre and Foufelle, 2007).

Lipogenesis and lipolysis

Triglyceride storage (lipogenesis) and breakdown (lipolysis) represent two major biological pathways in adipocytes (Ahmadian et al., 2007; Gregoire et al., 1998). Brown adipocytes possess a great capacity for uncoupled OXPHOS that results in the generation of heat. Contrarily, white adipocytes have reduced oxidative capacity as their main function is converting excess energy to store as triglycerides (Mottillo et al., 2014). For the process of lipogenesis, triglycerides can be synthesized from pre-existing FAs taken up from circulating triglycerides in the plasma or from non-lipid substrates such as carbohydrates (*de novo* lipogenesis) (Townsend and Tseng, 2014; Vázquez-Vela et al., 2008) (**Fig. 2**). Although FA synthesis occurs in the cytosol, mitochondria are essential for the generation of key metabolic intermediates, such as acetyl-CoA (Cedikova, 2016), that are required for lipogenesis (De Pauw et al., 2009). De novo lipogenesis begins with glucose metabolism to pyruvate, which is then converted into Acetyl-CoA in the mitochondria. Acetyl-CoA

enters the TCA cycle to form citrate, which would normally be used in the TCA cycle to produce isocitrate. However, in de novo lipogenesis, it crosses the inner mitochondrial membrane into the cytosol and is targeted for cleavage by ATP citrate lyase (ACL) generating acetyl-CoA and oxaloacetate (**Fig. 2**). Acetyl-CoA carboxylase (ACC) converts cytosolic acetyl-CoA to malonyl-CoA that is the first commitment step in FA synthesis (Mounier et al., 2014; Ferre and Foufelle, 2007). The lipogenic fate of malonyl-CoA is palmitate. This reaction is catalyzed by fatty acid synthase (FAS) which utilizes energy derived from NADPH. Some palmitate is then elongated to form stearate. Palmitate and stearate can be subsequently desaturated by stearoyl-CoA desaturase (SCD1) forming palmitoleate and oleate respectively. Desaturation is the formation of monounsaturated FAs from their respective substrates. These mono-unsaturated FA molecules form components of phospholipids that integrate into the lipid bilayer of the cell membrane or triglycerides for mobilization in very low density lipoproteins (Mounier et al., 2014). In addition, they can also be esterified to form triglycerides for storage (Ameer et al., 2014).

An opposite major function of adipose tissue is lipolysis, which is stimulated in energy deprivation conditions and non-shivering thermogenesis (Ahmadian et al., 2007, Vaillancourt et al., 2009) (**Fig. 3**). In this case, β-adrenergic agonists such as norepinephrine released by the sympathetic nervous system, bind to β-adrenergic receptors which activate a G_S (guanine nucleotide-binding) protein to initiate the cAMP/PKA-dependent pathway (Cole and Sood, 2012). The G_S protein activates adenylyl cyclase that converts ATP to cyclic AMP (cAMP) and leads to the activation cAMP-dependent protein kinase (PKA) (Collins and Surwit, 2001). PKA then phosphorylates the hormone sensitive lipase HSL (Stralfors and Belfrage, 1983) and perilipins that are essential for fat

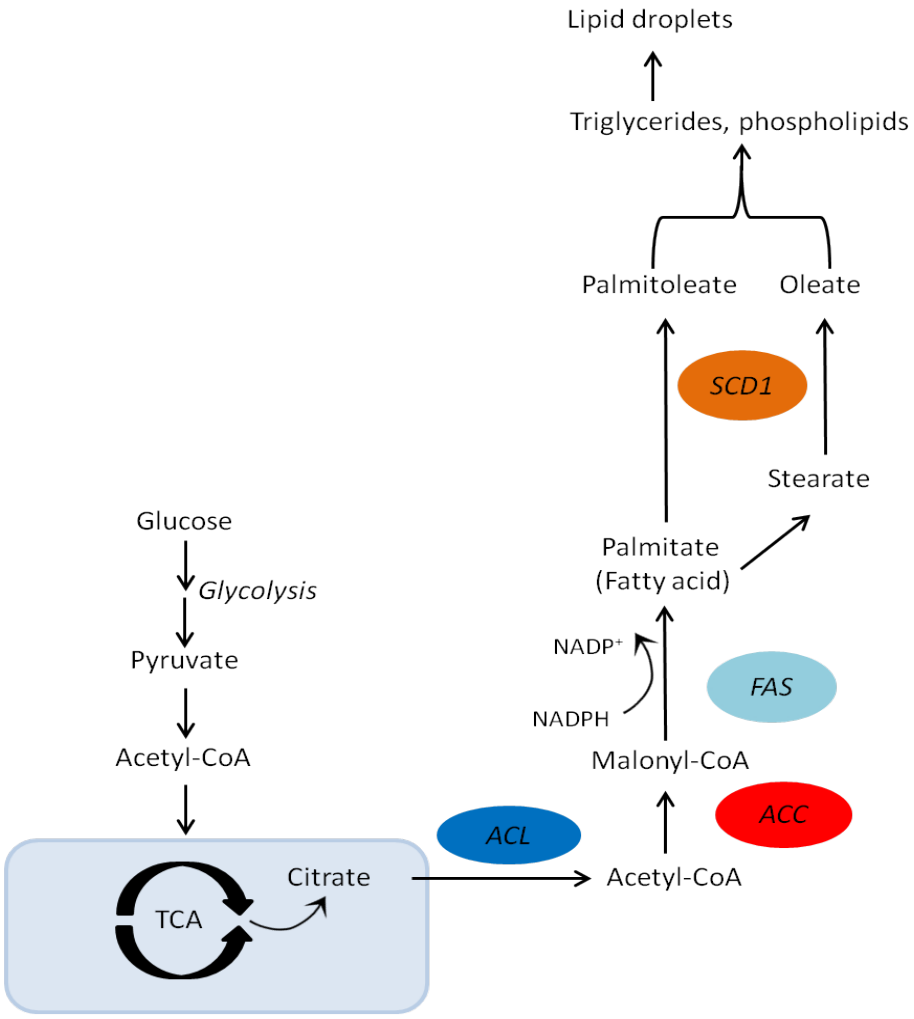

Figure 2. De novo lipogenesis in adipocytes. Glucose is metabolized into pyruvate via glycolysis, which then moves into the mitochondria where it is converted into acetyl-CoA. Acetyl-CoA enters the TCA cycle to form citrate, which has the ability to cross the inner mitochondrial membrane into the cytosol. In the cytosol, it is targeted for cleavage by ATP citrate lyase (ACL) generating acetyl-CoA. Acetyl-CoA carboxylase (ACC) converts cytosolic acetyl-CoA to malonyl-CoA. Malonyl-CoA is converted into palmitate by fatty acid synthase (FAS) which utilizes energy derived from NADPH. Some palmitate is elongated to form stearate. Palmitate and stearate are subsequently desaturated by stearoyl-CoA desaturase (SCD1) forming palmitoleate and oleate respectively. These mono-unsaturated fatty acid molecules form phospholipids or triglycerides for storage.

mobilization in adipose tissue (Greenberg et al., 1991; Egan et al., 1990). HSL phosphorylation activates its hydrolytic activity (Fredrikson et al., 1981) and subcellular translocation from the cytosol to the lipid droplet where it can begin to break down triglycerides (Egan et al., 1992; Clifford et al., 2000; Brasaemle et al., 2000). Triglycerides

are hydrolyzed sequentially by different lipases. In the first enzymatic reaction, triglycerides are broken down by adipose triglyceride lipase (ATGL) into diacylglycerol and a FA molecule. DAG is further hydrolyzed by hormone sensitive lipase (HSL) to yield monoacylglycerol and another FA molecule. MAG is subsequently hydrolyzed to release glycerol and FA (Duncan et al., 2007). FAs are broken down in the mitochondria mainly through β-oxidation, releasing acetyl-CoA which enters the TCA cycle which generates NADH and $FADH_2$, which are reducing agents utilized in the ETC (Aon et al., 2014).

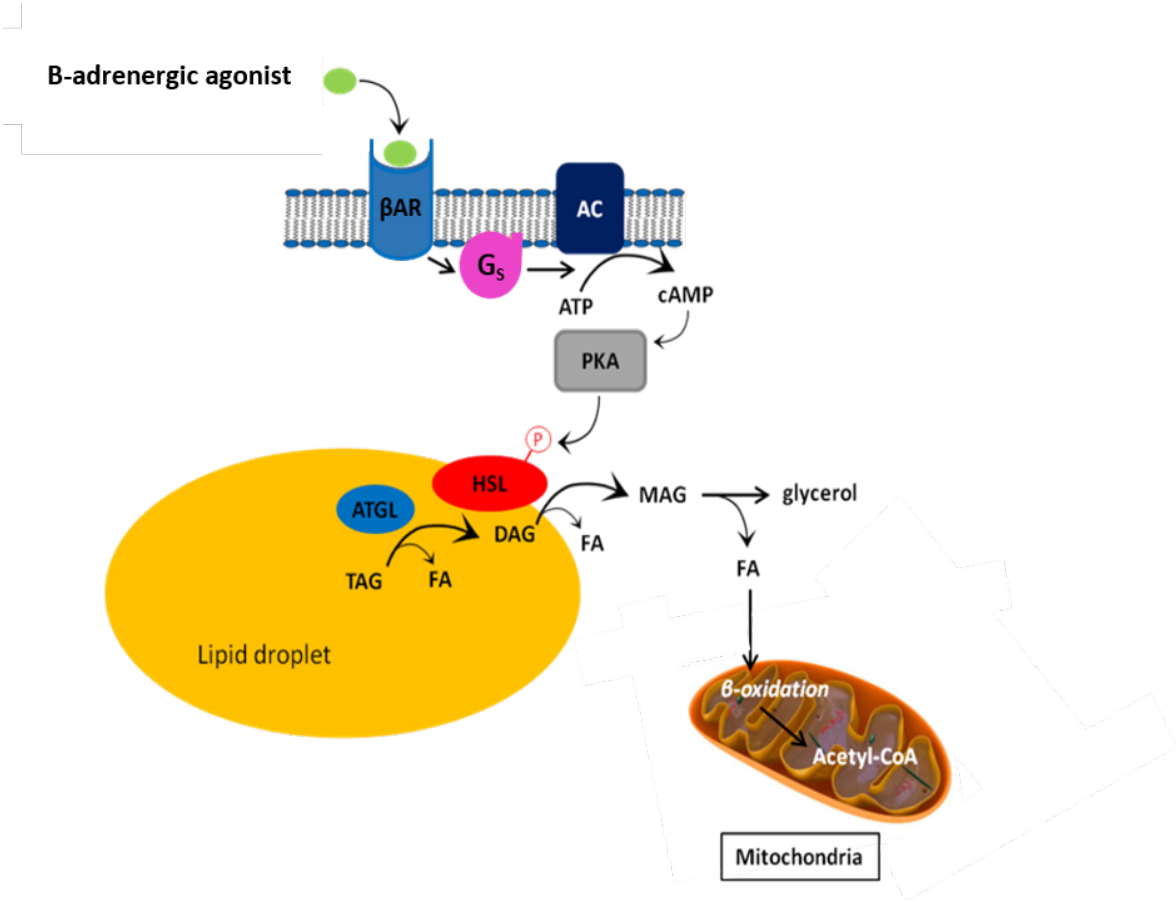

Figure 3. Lipolysis in adipocytes. β-adrenergic agonists bind to β-adrenergic receptors (βAR) and lead to the activation of a G_S protein. G_s activates adenylyl cyclase (AC) that converts ATP to cyclic AMP (cAMP). cAMP activates cAMP-dependent protein kinase (PKA) (Collins and Surwit, 2001). PKA then phosphorylates the hormone sensitive lipase (HSL). Triglycerides (TAG) are metabolized by adipose triglyceride lipase *(*ATGL*)* into diacylglycerol (DAG) and a free fatty acid molecule. DAG is further hydrolyzed by hormone sensitive lipase (HSL) to yield monoacylglycerol (MAG) and another FA. MAG is subsequently hydrolyzed to release glycerol and FA. FAs can enter the mitochondria where they are converted into acetyl-CoA mainly through β-oxidation.

Non-shivering thermogenesis

Exposure to cold temperatures imposes a metabolic challenge in mammals that must be met by maximizing their energy expenditure with heat production to ultimately restore homeothermy. Browning is the induction of brown and beige adipocytes to non-shivering thermogenesis during this challenge (Sanchez-Gurmaches et al., 2016; Kajimura et al., 2015; Fenzl and Kiefer, 2014; Bartelt and Heeren, 2014; Harms and Seale, 2013; Seale et al., 2009). This is accomplished by uncoupling protein-1 (Ucp-1) in the mitochondria that acts as a pore for protons re-entering the matrix thereby uncoupling OXPHOS. In their non-activated state, Ucp-1 in brown adipocytes is negatively regulated by purine nucleotides, primarily ATP (Nicholls, D.G., 1974; Cannon and Nedergaard, 2004; Kajimura and Saito, 2014). The inhibition of Ucp-1 allows coupled ATP-generation via OXPHOS (Fedorenko et al., 2012). However, in their activated state during exposure to cold temperatures, the sympathetic nervous system initiates the release of norepinephrine which binds the adrenergic receptors and triggers thermogenesis in brown and beige adipocytes (Cannon and Nedergaard, 2004) (**Fig. 3**). The adrenergic stimulation induces lipolysis and generates FA molecules which bind to and activate Ucp-1. Activation of Ucp-1 by FA molecules uncouples electron transport and ATP synthesis, resulting in the production of heat instead of ATP. In order to circumvent a potential energy crisis of low ATP generation, glycolysis is upregulated, as well as the TCA cycle (Cooney and Newsholme, 1982).

For browning in WAT, Ucp-1 expression in white adipocytes is negligible, but is expressed in beige adipocytes upon stimulation (Cedikova et al., 2016). Under basal conditions, beige adipocytes display comparable patterns of gene expression as white

adipocytes. However, upon adrenergic stimulation, the expression of pro-thermogenic fat marker genes and OXPHOS are upregulated, resembling the genetic signature of *bone fide* brown adipocytes (Park et al., 2014; Wu et al., 2012).

It is not clear if beige cells originate from existing white adipocytes (transdifferentiation), non-committed progenitors (de novo differentiation) or pre-existing non-activated beige cells (Harms and Seale, 2013). Vitali *et al*. showed evidence supporting the transdifferentiation of mature white adipocytes into beige adipocytes upon prolonged cold exposure or pharmacological treatment with adrenergic agonists (Vitali et al., 2012). This white to beige conversion, however, is not accompanied by an increase in the expression of the brown adipocyte determination factor, PRDM16 (Seale et al., 2008). More recently, other groups used a pulse-chase fate-mapping technique in mice to track adipogenesis during WAT browning (Wang et al, 2013). Their results demonstrated that the majority of beige adipocytes in the subcutaneous WAT depot arise from de novo differentiation of precursor cells, rather than from pre-existing adipocytes.

β-adrenergic activation in adipocytes

β-adrenergic receptors (βARs) are members of the G-protein-coupled receptor family (Collins and Surwit, 2001), which is among the largest and most diverse families of membrane receptors (Kroeze et al., 2003). Adipocytes express all three subtypes of βARs that are transcribed from different genes (Collins, 2012). Since βAR activation promotes lipolysis of triglycerides stored in both white and brown adipocytes, an in-depth understanding of the β-adrenergic signalling pathways may provide more insight into the manipulation of adipocytes to increase fat hydrolysis and reduce fat stores (Collins, 2012).

Earlier studies that were aimed to identify the functional differences between beige and brown adipocytes have shown conflicting data on the dispensability of β_3-adrenergic signalling for the browning of white adipocytes (de Jong et al., 2017). It was previously suggested that while brown adipocytes could respond to cold exposure in the absence of the β_3AR (Mattsson et al., 2011; Susulic et al., 1995), white adipocytes depended on β_3-adrenergic signalling for cold-induced development of beige adipocytes and concurrent transcriptional activation of thermogenic genes (Barbatelli et al., 2010; Jimenez et al., 2003). However, de Jong et al has recently shown that β_3-adrenergic signalling in white adipocytes is not absolutely critical for browning upon cold stimulation in contrast to earlier observations (de Jong et al., 2017). They found that β_3AR genetically deleted mice had a fully intact thermogenic gene program in both beige and brown adipose tissue during cold exposure. Thus, the requirement of the β_3ARs for cold-induced activation of thermogenic genes cannot be used as a factor to study the functional differences between beige and brown adipocytes (de Jong et al., 2017).

Several rodent models have been used to study lipolysis using the β_3-adrenergic agonist, CL 316,243 (CL) (Duteil et al., 2014; Himms-Hagen and Ghorbani, 1998; Collin and Surwit, 1996). Treatment with CL resulted in decreased lipid accumulation due to increased lipolytic activity in white adipocytes (Klaus et al., 2001). Interestingly, chronic CL treatment increases triglyceride turnover or lipolysis similarly in all adipose depots, despite drastic resulting differences in Ucp-1 (Mottillo et al., 2014). In the context of glucose metabolism, chronic treatment with CL has been demonstrated to up-regulate the expression of the insulin-sensitive glucose transporter GLUT4 in WAT and BAT of rats (Duffaut et al., 2006). Thus supporting the anti-diabetic properties of pro thermogenic

tissue activation (Bloom et al., 1992; Umekawa et al., 1997). Importantly, β_3-adrenergic stimulation in WAT of mice upregulates the expression of lysine-specific demethylase 1, which directly stimulates the expression of nuclear genes involved in OXPHOS (Duteil et al., 2014). However, the role of LSD1 in brown adipose tissue and its expression in response to β_3-adrenergic stimulation has not been investigated in great detail (Duteil et al., 2016).

CL binds to β_3ARs to activate the cAMP/PKA pathway mimicking cold exposure stimulation in non-shivering thermogenesis (Mouchiroud et al., 2014). Although it is widely accepted that lipolysis is stimulated by the cAMP/PKA pathway through HSL activation, there is increasing evidence supporting alternative intracellular signalling pathways that are activated through G-protein-coupled receptors. In adipocytes, the β_3AR can activate p38 mitogen-activated protein kinase (p38 MAPK) via PKA and p38 MAPK activity is essential for cAMP-dependent Ucp-1 transcription (Greenberg et al., 2001; Cao et al., 2001). CL has been shown to induce p38 MAPK activation in a dose- and time-dependent manner in both white and brown adipocytes. Altogether, these results elucidate the different downstream targets of the β_3-adregernic pathway, which ultimately lead to lipolysis and mitochondrial Ucp-1 transcription.

Insulin-induced lipogenesis in adipocytes

Insulin has been shown to be a critical hormonal factor in inducing de novo lipogenesis (Cederquist et al., 2017; Kersten, 2001) and inhibiting lipolysis through the PI3K/Akt pathway (Langin, 2006). Insulin binds to the insulin receptor and activates tyrosine kinase activity. This recruits glucose transporters to the membrane thereby

promoting glucose uptake by adipose tissue (Cederquist et al., 2017), as well as activates lipogenic enzymes via mTORC1 and the transcription factor sterol regulatory element binding protein-1 (SREBP-1), (Kersten, 2001). Insulin treatment simultaneously results in the activation of the antilipolytic enzyme phosphodiesterase 3B (PDE 3B) by Akt (Wijkander et al., 1998). PDE 3B reduces intracellular cAMP levels, resulting in lowered activity of PKA and ultimately the deactivation of HSL, thereby inhibiting lipolysis (Wijkander et al., 1998).

From a disease perspective, insulin or insulin resistance plays a pivotal role in metabolic disorders such as obesity and type 2 diabetes (Smith and Kahn, 2016). Under normal physiological conditions, lipogenesis and lipolysis are carefully regulated within adipose tissues and in concert with other systemic organs, especially the liver. Insulin-resistant obesity results in impaired inhibition of lipolysis and consequently, increased release of FAs and glycerol (Perry et al., 2015; Arner and Langin, 2014). Ultimately, this can lead to ectopic lipid accumulation and dyslipidemia (Gustafson and Smith, 2014; Abraham et al., 2015).

Regulation of mitochondrial DNA in adipocytes

Although majority of protein-encoding genes are found within the nucleus, mitochondria also contain their own DNA (mtDNA), which is derived from a separate evolutionary origin than the nuclear genome (Gray et al., 1999). The human mitochondrial genome spans 16.6-kbp and contains a total of 37 genes that encode 13 mitochondrial proteins, 22 mitochondrial tRNAs, and 2 mitochondrial rRNAs (Anderson et al., 1981) (**Fig. 4**). The mouse mitochondrial genome exhibits a high level of similarity to that of

humans (Gray, 2012). The 13 mitochondrial-encoded proteins are functional components of the ETC for OXPHOS. These components, which are absolutely required for electron transit and ATP production, are subunits of the ETC complexes I, III, IV, and V (Schon et al., 2012). This is highlighted by ATP6 and ATP8 that are two critical subunits of complex V (ATP Synthase). Together they form a major component of the ATP Synthase, the F_0 structural domain, consisting of the membrane proton channel through which protons pass to produce ATP from ADP (Grzybowska-Szatkowska et al., 2014). Thus, without subunits ATP6 and 8, the synthase cannot support the energetically favorable flow of protons across the inner mitochondrial membrane to form ATP.

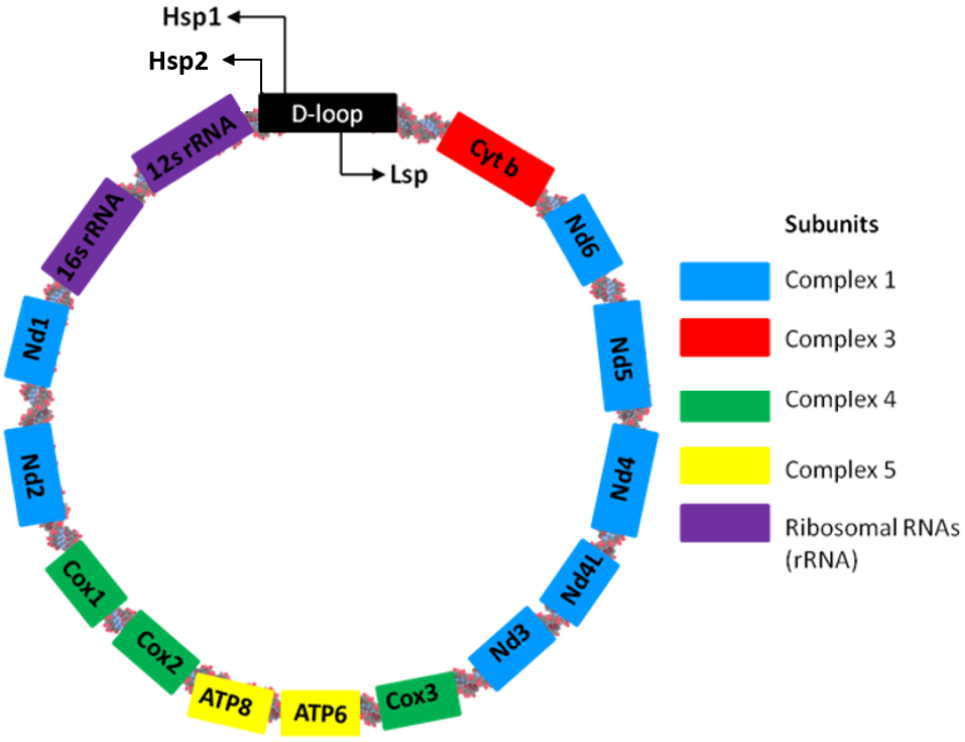

Figure 4. Mouse and human mitochondrial-encoded genes. The human and mouse mitochondrial DNA (mtDNA) is a closed double-stranded circular DNA, with genes located on both strands, which are referred to as the heavy (H) and light (L) strands. The H-strand contains two promoters, Hsp1 and Hsp2, whereas the L-stand contains a single promoter, Lsp, located in the D-loop regulatory region. Thirteen mitochondrial protein subunits of complexes I, III, IV, and V are encoded from the mtDNA and are functional components of the ETC absolutely required for OXPHOS.

The structure of mtDNA is a closed double-stranded DNA circle with genes located on both strands, which are referred to as the heavy (H) and light (L) strands based on their relative densities upon gradient centrifugation. The H-strand contains two promoters, heavy strand promoter 1 and 2 (Hsp1 and Hsp2), while the L-strand contains a single promoter, light strand promoter (Lsp). Transcription can initiate in either direction along the circular genome at any one of the three promoters. Hsp1 and Hsp2 are located 100 bp apart within the D-loop region and transcribed in the same direction (Martin et al., 2005). Hsp2 and Lsp derived transcripts yield polycistronic messages that are subsequently processed and modified. On the other hand, Hsp1 terminates after transcribing 12S and 16S rRNAs (Peralta et al., 2012; Kruse et al., 1989; Martin et al., 2005).

The transcription of mitochondrial genes involved in OXPHOS and other mitochondrial processes is tightly controlled by key mitochondrial and nuclear factors that can interact directly with the mtDNA. Pgc-1α is a master regulator of mitochondrial biogenesis (Jornayvaz and Shulman, 2010; Wu et al., 1999). It interacts with and activates the nuclear transcription factors 1 and 2 (NRF-1 and NRF-2), leading to the transcription of the mitochondrial transcription factor (Tfam). Tfam translocates into the mitochondria where it activates the transcription and replication of mtDNA by binding to the D-loop (Ventura-Clapier et al., 2008). In brown adipocytes that are abundant with mitochondria and express high levels of Ucp-1 relative to white adipocytes, β-adrenergic signalling activates the expression of Pgc-1α, which increases the expression of Ucp-1 and mitochondrial genes (Fernandez-Marcos and Auwerx, 2011; Puigserver et al., 1998). Furthermore, cold-induced brown adipocytes increase in Ucp-1 expression concurrently

with activated mitochondrial biogenesis (Cohen and Spiegelman, 2015). Moreover, adipose-specific TFAM genetically deleted mice demonstrated a significant reduction in mtDNA copy number and a down regulation of OXPHOS proteins (Vernochet et al., 2012). As a result, both WAT and BAT displayed decreased complex I and complex IV enzymatic activities (Wredenberg et al., 2006). A recent study showed that a splicing isoform of Pgc-1α, NT-Pgc-1α, also has a direct regulatory effect on mtDNA transcription in brown adipocytes, as its selective expression in Pgc-1α genetically deleted brown adipocytes resulted in higher expression of mtDNA-encoded genes (Chang and Ha, 2017).

The mitochondrial transcription termination factor (mTERF) protein family has also been identified as key transcriptional regulators of the mitochondrial genome (Roberti et al., 2006). mTERF1 is widely believed to mediate the transcription termination of a shorter transcript derived from the HSP1 promoter by binding to the termination region and facilitating DNA unwinding (Roberti et al., 2006;Yakubovskaya et al., 2010). However, their role in adipose tissue is unknown.

Rb family and adipocyte metabolism

The retinoblastoma susceptibility gene family proteins, Rb, Rbl1 (p107) and Rbl2 (p130), have been best described by their nuclear function as molecular repressors of mammalian cell growth and proliferation (Balciunaite et al., 2005). Rb is expressed in both proliferating and non-proliferating cells, while p130 is expressed in differentiated or quiescent cells and p107 is prominently expressed in proliferating cells (Macaluso et al., 2006). Each Rb family member is known to interact with distinct proteins of the E2F family of transcription factors, thereby recruiting chromatin remodeling enzymes such as histone

deacetylases and histone methyltransferases, which in turn repress the expression of genes involved in cell cycle progression, as well as differentiation and development (Caputi et al., 2005; Cobrinik, 2005).

Interestingly, our lab has recently shown that p107 plays a pivotal role in dictating adipocyte progenitor fate by regulating metabolism (Porras et al., 2017; De Sousa et al., 2014). In the absence of p107, glucose metabolism is directed to lactate, as an alternative to the TCA cycle. This metabolic profile was found to control the differentiation of brown versus white adipocytes.

Unlike p107, little is known about the function of homologous family member p130 in adipocyte progenitors and their differentiated progeny (Porras et al., 2017; De Sousa et al., 2014; Ross et al., 2007). Several genome-wide association studies (GWAS) have discovered hundreds of genetic loci with powerful associations for over 300 diseases, including at least 75 obesity-susceptibility loci (Day and Loos, 2011; Lu and Loos, 2013). The FTO (fat mass and obesity associated gene locus) was recognized as the locus with the most significant impact on body mass index (BMI) and the disposition of developing obesity (Lu and Loos, 2013) (Frayling et al., 2007; Scuteri et al., 2007). Common single nucleotide polymorphisms (SNPs) occur in the intronic regions of the FTO locus in close proximity to different genes (Davies et al., 2013). These SNPs can alter susceptibility to obesity by interfering with the expression or function of the nearby genes, one of which include p130. Interestingly, the obesity-risk allele of a common GWAS SNP in intron 1 of the FTO gene was concomitant with increased p130 expression in peripheral blood lymphocytes (Jowett et al., 2010).

2. RATIONALE AND OBJECTIVES

Rationale

As p130 is expressed only in adipocytes and nearly undetectable in their proliferating progenitor cells, the rationale for this project is to establish a metabolic role for p130 in terminally differentiated adipocytes.

Hypothesis

In adipocytes, p130 functions by regulating fatty acid metabolism.

Objectives

1. To identify a metabolic role for p130 in white and brown adipocytes.
2. To investigate the molecular function of p130 in de novo lipogenesis.
3. To investigate the molecular function of p130 in lipolysis.

3. MATERIALS AND METHODS

Mice and Dissections

All animal experiments were performed according to the guidelines approved by the Animal Care Committee of York University. Experiments were performed on adult (8–16-week old) mice of the Balb/c genetic background. Mice were injected with 1 mg/kg β_3-adrengeric agonist CL 316,243 (Tocris Bioscience, Bristol, UK, https://www.tocris.com/) diluted in saline, 0.6 units/kg insulin or PBS intraperitoneally. Brown and white adipose depots were dissected at varying time points for analysis.

Cell Types and Tissue Culture

C3H10T1/2 cells are an uncommitted embryo cell line derived from 14 to 17 day-old C3H mouse embryos obtained from the American Type Culture Collection. Cell lines for p130 KD and scrambled control were derived by transfecting C3H10T1/2 cells with plasmid expressing short hairpin (sh) RNAi (TRCN0000071274) or control empty vector (Sigma-Aldrich, St. Louis, Missouri, http://www.sigmaaldrich.com), respectively. After 24 hours, cells were washed and cell lines were selected based on their survival in 1.5 μg/ml puromycin. Murine embryonic fibroblasts representing a rich source of primary mesodermal stem cells were isolated from embryos of heterozygous p130 genetically deleted mating pairs at 14.5 days post coitum. After embryos were isolated and the placenta removed, ectodermal and endodermal cells of the head, tail and internal organs were discarded and the remaining mesodermal tissue was minced and plated. All cells

were grown in low glucose media (5.5mM Dulbecco's Modified Eagle's Medium (DMEM) (Wisent Bioproducts ST-BRUNO, Quebec, http://www.wisentbioproducts.com) with 10% fetal bovine serum (FBS) and 1% penicillin/streptomycin.

Cells were differentiated to adipocytes after reaching confluency (day 0). At day 0, the growth media was supplemented with 0.5mM isobutylmethylxanthine, 125 nm indomethacin, 1μM dexamethasone, 850 nM insulin, 1 nM tri-iodothyronine (T3), and 1μM rosiglitazone for 2 days. At day 2, cells were switched to maintenance media that contained 850 nM insulin, 1 nM T3, and 1μM rosiglitazone for 6 days. At day 9, some plates were treated with 5 or 10 μM rosiglitazone (Sigma-Aldrich, St. Louis, Missouri, http://www.sigmaaldrich.com) and 10 or 40 μM CL 316,243 (Tocris Bioscience, Avonmouth, Bristol, United Kingdom, https://www.tocris.com) for 24 hours. Plates were subsequently washed with PBS and used for mitochondrial, RNA or protein isolation as described below.

Stromal Vascular, Adipocyte and Tissue Isolation

White and brown fat pads from mice were dissected from the inguinal and interscapular regions, respectively. Tissues were minced and digested in Krebs-Henseleit Buffer Modified medium (Sigma-Aldrich, St. Louis, Missouri, http://www.sigmaaldrich.com) containing 1mg/mL collagenase I (Sigma-Aldrich, St. Louis, Missouri, http://www.sigmaaldrich.com). Samples were rocked on a platform shaker at 80 rpm in 37°C for 30 minutes. Digested tissue was passed through a 100 μm

sterile nylon mesh filter to collect the stromal vascular fraction and adipocytes. To separate the stromal vascular fraction from the fatty layer containing adipocytes, the filtered cells were centrifuged at 1500 rpm for 5 minutes. The top fatty layer now containing adipocytes was carefully transferred to a new tube. Adipocytes were subsequently suspended in 10mL of low glucose media and might be treated with 40 μM CL 316,243 for 5 hours or 850 nM insulin for 30 minutes.

For whole tissue protein isolation, fat pads were lysed directly in RIPA lysis buffer (0.1% sodium deoxycholate, 0.5% NP-40, 5 mM EDTA, 50 mM Tris HCL pH 7.5, 150 mM NaCl,) on a cell disruptor (Retsch MM400) for 2.5 minutes (frequency 30 Hz with 30s on and 30s off). After disruption, the supernatant was centrifuged at 15000 rpm for 15 minutes at 4°C. The supernatant was collected and used for Western blot analysis.

Mitochondrial Isolation

C3H10T1/2 cells, their differentiated progeny, isolated primary stromal vascular cells or primary adipocytes were washed twice with PBS and pelleted by centrifugation at 1500 rpm for 5 minutes. The pellet was dissolved in mitochondrial isolation buffer (0.25 M sucrose, 0.1% BSA, 0.2 mM EDTA, 10 mM HEPES) containing protease inhibitors (1 mg/ml of each of pepstatin, aprotinin and leupeptin) and transferred into a pre chilled Dounce homogenizor. The sample was homogenized using loose (6 complete turns) and tight (6 complete turns) glass rods. The homogenate was transferred into an eppendorf tube and centrifuged at 1000 g at 4ºC for 10 minutes. The supernatant was collected and the pellet containing the debris and nucleus were discarded. The supernatant was

centrifuged at 14000 g for 15 minutes at 4ºC and the resulting supernatant was saved as the cytoplasmic fraction. The pellet representing the mitochondrial fraction was washed twice and dissolved in 30 ul of isolation buffer. The mitochondria were lysed by repeated freeze-thaw cycles (3 times each) on dry ice.

Nuclear-Cytoplasmic Isolation

White and brown fat pads from mice aged 4-5 weeks were dissected from the inguinal and interscapular regions, respectively. The tissue was lysed directly in 500 µL cytoplasmic lysis buffer (10 mM Tris pH 7.4, 10 mM NaCl, 3 mM $MgCl_2$, 0.5% NP-40 and protease inhibitors) on the cell disruptor for 2.5 minutes (frequency 30 Hz with 30s on and 30s off). After disruption, the supernatant was transferred to a new tube and incubated on ice for 5 min followed by rocking at 4°C for 5 min. After incubation, a small volume (150 µL) of the homogenate mixture was removed. This fraction represented the "whole cell lysate". The remaining homogenate was then centrifuged at 2500 g for 5 min at 4^oC. The supernatant, which represented the cytoplasmic extract, was then transferred to a clean pre-chilled tube. The cell pellet containing intact nuclei was then washed with the cytoplasmic lysis buffer. After 10 washes, the insoluble cell pellet was lysed with nuclear lysis buffer (50 mM Tris pH 7.4, 5 mM MgCl2, 0.1 mM EDTA, 1mM dithiothreitol (DTT), 40% (wt/vol) glycerol containing 0.15 unit/ul benzonase nuclease (sc-202391, Santa Cruz Biotechnology, Dallas, Texas, United States, https://www.scbt.com/scbt/home) to digest the DNA and RNA in the suspension.

Western Blot Analysis

Protein samples to be loaded were first boiled for 3 minutes in loading buffer containing 4% SDS, 10% 2-mercaptoethanol, 20% glycerol, 0.004% bromophenol blue, 0.125 M Tris-HCl and 1 mM DTT. Samples were loaded on gradient (6-15%) or 7.5% polyacrylamide gels in running buffer (25 mM Tris-base, 192 mM glycine and 0.1% SDS) and the proteins were separated by electrophoresis for 1.5 hours at 30 milliamps. Proteins were transferred on a 0.22 μm pore size nitrocellulose membrane (Santa Cruz Biotechnology, Dallas, Texas, United States, https://www.scbt.com/scbt/home) at 4ºC for 80 minutes at 100V, using a wet transfer method (50 mM Tris-base, 384 mM glycine, 20% methanol). The membranes were blocked for an hour at room temperature in 5% milk in TBST (150 mM NaCl, 50 mM Tris base and 0.1% Tween-20). Membranes were probed with primary antibodies diluted in 5% milk in TBST overnight at 4ºC with gentle rocking. Antibodies used were rabbit polyclonal anti-p130 (sc-317X, Santa Cruz Biotechnology, Dallas, Texas, United States, https://www.scbt.com/scbt/home), rabbit polyclonal anti-Cox4 (ab16056, Abcam, Cambridge, United Kingdom, http://www.abcam.com/) and monoclonal anti-α-tubulin (T9026, Sigma, St. Louis, Missouri, http://www.sigmaaldrich.com). The membranes were then washed three times with TBST and secondary antibodies conjugated with horseradish peroxidise diluted in 5% milk in TBST were added and incubated for an hour at room temperature with gentle rocking. Secondary antibodies were goat anti-rabbit and goat anti-mouse (Bio-rad Laboratories, Mississauga, Ontario, http://www.bio-rad.com/). The membranes were then washed 3 times with TBST for 5 minutes each followed by a final wash with TBS for 10 minutes. The membranes were visualized with normal (Pierce, Carlsbad, California,

United States, https://www.thermofisher.com/ca/en/home.html) and highly sensitive (Immobilon Western Chemiluminescent HRP Substrate, Millipore, Darmstadt, Germany, http://www.emdmillipore.com/CA/en) chemiluminescence reagents on photographic film (Santa Cruz Biotechnology, Dallas, Texas, United States, https://www.scbt.com/scbt/home). Protein levels were then evaluated through densitometry using Image J software.

Quantitative Chromatin Immunoprecipitation Assay (qChIP)

Isolated mitochondria were re-suspended in 200 µL PBS with 1% formaldehyde and rocked at RT for 10 minutes to enable the crosslinking/fixation reaction. This was quenched by adding 200 µL of 125 mM glycine in PBS and rocking for 5 minutes at RT. 400 µL of cold PBS with 1 mM NaF and 100 mM Na_3VO_4 was then added and the cross-linked mitochondria were centrifuged at 14,000g for 5 minutes at 4°C. The supernatant was discarded and the pellet was washed again by centrifugation in 400 µL in the same buffer. The pellet was re-suspended in 500 µL of chromatin immunoprecipitation (ChIP) Lysis Buffer (40 mM Tris pH 8.0, 1% Triton X-100, 4 mM EDTA, 300 mM NaCl, 1µg/ml each of protease inhibitors [pepstatin A, aprotinin, leupeptin], 1 mM phenylmethylsulfonyl fluoride [PMSF] and 1mM Na_3VO_4) and kept on ice until sonication. Samples were sonicated at 12 cycles of 15s on, 45s off, amplitude 15. Post sonication, samples were centrifuged at 13,000 rpm for 10 minutes at 4°C. The supernatant was transferred to a new tube and an equal volume of Dilution Buffer 1 (40 mM Tris pH 8.0, 4 mM EDTA, 1 µg/ml of each protease inhibitors, 1 mM PMSF and 1

mM Na_3VO_4) was added. 20 µL was removed and added to 100 µL of Dilution Buffer 2 (Dilution Buffer 1 with 0.5% Triton X-100 and 150mM NaCl) and stored as Input DNA at -20°C. The remaining sample was diluted to 750 µL with Dilution Buffer 2. 50 µL of Protein A/G agarose beads (Santa Cruz Biotechnology, Dallas, Texas, United States, https://www.scbt.com/scbt/home) were added and the sample pre cleared by rocking at 4°C for 1 hour. The beads were pelleted by centrifugation at 1500 rpm for 2 minutes in 4°C and the supernatant transferred into another tube. The supernatant was incubated overnight on a rocker at 4°C with 5 µg of rabbit polyclonal p130 antibody (sc-317X, Santa Cruz Biotechnology, Dallas, Texas, United States, https://www.scbt.com/scbt/home).

The next day 50 µL Protein A/G agarose beads were added to the sample and rocked at 4°C for 90 minutes. Beads were pelleted by centrifugation (1500 rpm, 2 minutes, 4°C) and the supernatant containing unbound protein/DNA was discarded. The agarose bound antibody/protein/DNA was washed on a rocking platform with 1 mL of various wash buffers for 5 minutes each. Beads were pelleted at 1500 rpm, 4°C, 2 minutes in between washes. The various wash buffers were in sequence: Low Salt Immune Complex Wash Buffer (0.1% SDS, 1% Triton X-100, 2 mM EDTA, 20 mM Tris-HCl pH 8.2, 150 mM NaCl), High Salt Immune Complex Wash Buffer (0.1% SDS, 1% Triton X-100, 2 mM EDTA, 20 mM Tris-HCl pH 8.2, 500 mM NaCl), LiCl Immune Complex Wash Buffer (0.25 M LiCl, 1% IGEPAL-CA630, 1% deoxycholic acid, 1 mM EDTA, 10 mM Tris pH 8.1), and two TE Buffer washes (10 mM Tris-HCl, 1mM EDTA pH 8.0).

After the last wash, the pellet was re-suspended in 250 µL of fresh Elution Buffer (1% SDS, 0.1 M $NaHCO_3$), vortexed and placed on a rotator for 15 minutes at RT. Samples were spun down at 1500 rpm for 2 minutes and the supernatant transferred to another tube. 250 µL of Elution Buffer was re-added to the pellet and the previous step repeated. The eluates were combined (final volume of 500 µL). To reverse crosslinks 20 µL of 5 M NaCl was added to the combined eluates and 4 µL to the Input DNA and incubated at 65°C for 6 hours. The DNA was purified using a DNA Purification Kit (Active Motif, Carlsbad, California, https://www.activemotif.com/) as per manufacturer's instructions. DNA binding was then detected using qPCR as described below.

qPCR Analysis

qPCR experiments were evaluated following the MIQE (Minimum Information for Publication of Quantitative Real-Time PCR Experiments) guidelines (Bustin et al., 2009). For RNA isolation, Trizol reagent (Ambion by Life Technologies, Carlsbad, California, United States, https://www.thermofisher.com/ca/en/home.html) was used according to the manufacturer's instructions. 1 µg of RNA was reverse transcribed into cDNA using an All-in-One cDNA Synthesis SuperMix (bikmake, Houston, TX, http://www.bimake.com/) and the cDNA used for qPCR. The optical density (OD) of RNA was measured using the NanoDrop 2000 (Thermo Scienfic, Carlsbad, California, United States, https://www.thermofisher.com/ca/en/home.html) RNA purity was inferred by the A260/280 ratio (~1.80 is pure). qPCR assays were performed on Light cycler 96 (Roche, Missisauga, Canada, http://www.rochecanada.com/) using SYBR green Fast

qPCR Master mix (Biotool, Carlsbad, California, United States, https://www.thermofisher.com/ca/en/home.html) with appropriate primer sets and Rplp0 (36B4) as a normalization control (**Table 1**). Relative expression of cDNAs was determined after normalization with 36B4 using the ΔΔCt method. For qChIP, relative binding was determined by amplifying isolated DNA fragments using the D-loop primers and analysed using the ΔΔCt method. For fold change, ΔΔCt values were normalized to the control.

Microscope analysis

Cells were imaged using the ZEISS Axio Vert. A1 scope with 5X/0, 15 Ph1 objective (Carl Zeiss Canada, Toronto, Canada, https://www.zeiss.ca). Digital images were captured using a 12-megapixel camera. Lipid droplets were quantified manually using Microsoft paint.

Table 1. Primer sets used for qPCR

Gene Name	Sequence Accession Number	Amplicon Length (bp)	Forward primer sequence	Reverse primer sequence
Rplp0 (36B4)	MGI:1927636	29	GAG GAA TCA GAT GAG GAT ATG GGA	AAG CAG GCT GAC TTG GTT GC
mt-Nd4 (Nd4)	MGI:102498	66	CCT CAC ATC ATC ACT CCT ATT CTG	GGC TAT AAG TGG GGA AGA CCA TTT G
mt-Co2 (Cox 2)	MGI:102503	98	AGT TGA TAA CCG AGT CGT TCT G	CTG TTG CTT GAT TTA GTC GGC
mt-Atp6 (Atp6)	MGI:99927	55	TCC CAA TCG TTG TAG CCA TC	TGT TGG AAA GAA TGG AGT CGG
D-loop	MF 133498.1	173	GCG TTA TCG CCT CAT ACG TT	GGT GCG TCT AGA CTG TGT G

4. RESULTS

p130 is expressed in WAT and BAT in vivo and in vitro

To begin to study the potential metabolic role of p130 in adipocytes we ascertained that it was expressed in white and brown fat pads. Western blotting of tissue lysates of WAT and BAT revealed that p130 was expressed in both types of fat **(Fig. 5A)**. Furthermore, as p130 is well characterized as nuclear transcriptional co-repressor (Balciunaite et al., 2005), we confirmed its expression in the nuclear fractions of both tissues **(Fig. 5B)**.

As p130 was expressed in both white and brown adipocytes in vivo, we next assessed its expression in vitro. We first confirmed that C3H10T1/2 cell lines were sufficient for studying p130 by comparing p130 protein expression patterns during proliferation and at growth arrest (**Fig. 6A)**. As expected, Western blotting showed that p130 was virtually undetected in proliferating progenitors, but was expressed in growth arrested cells (**Fig. 6B**). This data is in accordance with what is in the literature providing a reasonable progenitor cell population to study p130 during in vitro adipocyte differentiation (Richon et al., 1997).

p130 regulates terminal adipocyte differentiation

We next assessed the importance of p130 function during adipocyte differentiation. For this, we generated a p130 knockdown (KD) in C3H10T1/2 cells by transfecting a plasmid to deliver a short hairpin RNA targeting p130 mRNA and control cells with empty vector. Cells were selected based on their survival in puromycin. Western blot analysis of the p130 KD cells showed a greater than 90% reduction of p130 protein levels compared to

control cells **(Fig. 7A and B)**. Interestingly, at day 9 of differentiation p130 KD cells showing drastically reduced numbers of lipid containing cells compared to the control **(Fig. 7C).**

p130 is expressed in the mitochondria of differentiating progenitors and adipocytes

As a substantial amount of p130 is present in the cytoplasm of BAT and WAT (**Fig. 5B)**, we assessed if p130 was present in the mitochondria. Intriguingly, protein expression analysis by Western blotting of primary white and brown adipocytes isolated from WAT and BAT of mice revealed that p130 was present in the mitochondria, and to a lesser extent in the cytoplasm **(Fig. 8A)**. We next determined if p130 had a potential mitochondrial role during adipocyte differentiation of C3H10T1/2 cells by Western blotting (**Fig. 8B**). A time course of adipocyte differentiation showed that during growth arrest at day 0 before the differentiation cocktail was added, p130 was localized in the mitochondria at low levels and decreased over time relative to the mitochondrial control, Cox IV **(Fig. 8C).** Together this data suggests a potential metabolic role for p130 that involves the mitochondria during differentiation of progenitors and then terminally differentiated adipocyte progeny.

De novo lipogenesis increases p130 mitochondrial localization in vitro

As the mitochondria play a key role in providing the metabolic substrates for de novo lipogenesis, we evaluated the potential involvement of p130. For this, we stimulated de novo lipogenesis by mimicking a carbohydrate-rich environment in vitro by adding 100mM glucose to differentiated C3H10T1/2 adipocytes. Western blotting analysis

revealed that glucose treatment in day 9 differentiated C3H10T1/2 adipocytes significantly increased mitochondrial p130 protein levels (**Fig. 9A and B**). Similarly, treatment with rosiglitazone, a PPAR-γ agonist and potent activator of lipogenesis (Festuccia et al., 2009), also resulted in significantly increased p130 protein levels in the mitochondria of differentiated C3H10T1/2 adipocytes (**Fig. 10A and B**). Further analysis revealed that increasing concentrations of rosiglitazone was associated with increasing levels of p130 in the mitochondria of adipocytes (**Fig. 10C**). Together, these findings provide compelling evidence linking the presence of p130 in the mitochondria with de novo lipogenesis in adipocytes.

Insulin-induced de novo lipogenesis increases p130 mitochondrial localization in vivo

We wanted to confirm that a physiologically induced system of de novo lipogenesis also influenced p130 mitochondrial localization. We performed this experiment two ways – in vivo and ex vivo. Insulin injection in mice stimulates de novo lipogenesis within 30 minutes (Shao et al., 2012). Thus, mice were injected with insulin to assess the subcellular localization of p130. After 30 minutes, mitochondria from white adipocytes were isolated from inguinal WAT for Western blotting analysis. Importantly, we found substantially increased p130 protein levels in the mitochondria of white adipocytes (**Fig. 11A**). We confirmed our in vivo data by Western blotting of ex vivo insulin treated white adipocytes (**Fig. 11B)**. Importantly, mitochondrial p130 protein levels were drastically higher than cytoplasmic levels in both experiments.

Fasting decreases p130 mitochondrial localization in primary brown adipocytes

We next examined if a physiological setting that induces lipolysis would also affect p130 mitochondrial function. Physiologically, overnight fasting induces lipolysis while decreasing lipogenesis in adipose tissue, resulting in a net loss of stored triglycerides (Ahmadian et al., 2007, Vaillancourt et al., 2009). We thus subjected adult mice to an overnight fast of 18 hours and analyzed brown adipocytes for Western blotting. Our results revealed decreased mitochondrial p130 localization in brown adipocytes of fasted mice compared to non-fasting mice (**Fig. 12).** This data suggests that decreased levels of p130 in the mitochondria of brown adipocytes may function during lipolysis opposite to how it functions in de novo lipogenesis.

Adrenergic agonist has opposing effects on p130 in brown and white adipocytes

In order to further elucidate the mitochondrial role for p130 in adipocytes we used a β_3-adrenergic agonist, CL 316,243 (CL), which is a known activator of triglyceride lipolysis in adipocytes (Klaus et al., 2001). Unexpectedly, Western blotting analysis revealed that CL treatment substantially increased mitochondrial p130 protein levels in isolated primary brown adipocytes isolated from mice injected with CL for 5 hours (**Fig. 13A).** As a means to show that increased mitochondrial p130 levels were due to a cell autonomous effect, we treated primary brown adipocytes with CL for 5 hours. We found higher protein levels of p130 in the mitochondria of treated compared to untreated cells, with the same effect as insulin (**Fig. 13B and 13C)**. Contrarily, as expected in the primary white adipocytes, we found p130 was regulated oppositely CL treatment abolished its mitochondrial localization (**Fig. 14A)**. Furthermore, we confirmed this

results by increasing concentrations of CL in differentiated white C3H10T1/2 adipocytes, which resulted in drastically decreasing mitochondrial p130 proteins levels compared to untreated cells **(Fig. 14B)**. Thus, CL that induces lipolysis has the opposite effect in white and brown adipocytes for the subcellular localization of p130.

p130 binds at the D-loop regulatory region of mitochondrial DNA

To study the importance of p130 localization in the mitochondria, we next investigated if it interacts with mtDNA, specifically the D-loop regulatory region containing the HSP1 and LSP1 promoters (Martin et al., 2005). For this we used a quantitative chromatin immunoprecipitation (qChIP) assay. Although conventionally used as the standard detection technique for interactions between protein factors and nuclear DNA, it can be readily adapted to mitochondrial studies (Leigh-Brown et al., 2010)**.** We evaluated the mitochondria of proliferating C3H10T1/2 cells as a negative control where p130 is absent and their terminally differentiated progeny where it is present in the mitochondria **(Fig. 6B)**. ChIP showed that p130 did not interact with mtDNA of proliferating progenitors, but it interacted with the D-loop region in terminally differentiated adipocytes **(Fig. 15).**

We next assessed if inducing de novo lipogenesis in vivo, that increases p130 protein levels in the mitochondria (**Fig. 11 and Fig. 13C**), influenced its interaction with mtDNA. Accordingly, we injected mice with insulin for 30 minutes and isolated mitochondria from white and brown adipocytes from WAT and BAT respectively. We analyzed promoter binding with D-loop primer sets amplifying amino acid residues 444 to 616 of the D-loop region. qChIP analysis of the mitochondria from white and brown

adipocytes demonstrated increased p130 binding to the D-loop region with insulin treatment compared to untreated cells (**Fig. 16A and 16B)**.

Furthermore, adrenergic stimulation that induces lipolysis in white adipocytes and drives p130 out of the mitochondria (**Fig. 14**), showed significantly reduced p130 interaction at the D-loop (**Fig. 17).** This data suggests that p130 might function as a transcriptional co-repressor of mtDNA, similar to the mechanism through which it represses nuclear DNA.

p130 interaction at the mtDNA is associated with mitochondrial gene transcription

To investigate the effect of p130 interacting at the D-loop of mtDNA we analyzed the expression of mitochondrial-encoded OXPHOS genes in vivo. Mice were fasted overnight for 18 hours and the mRNA from brown adipocytes were examined for qPCR analysis. Fasting, which induces lipolysis and diminished p130 levels in the mitochondria (**Fig. 12)**, resulted in markedly increased expression for mitochondrial-encoded OXPHOS genes *Nd4* (Complex 1), *Cox2* (Complex 4) and *Atp6* (Complex 5) **(Fig. 18)**. Together, this data suggests that p130 may function in adipocyte metabolism as a mitochondrial co-transcriptional repressor by binding to the D-loop region and down regulating mitochondrial-encoded OXPHOS genes.

Figure 5

A

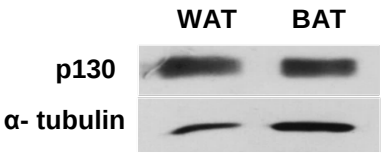

B

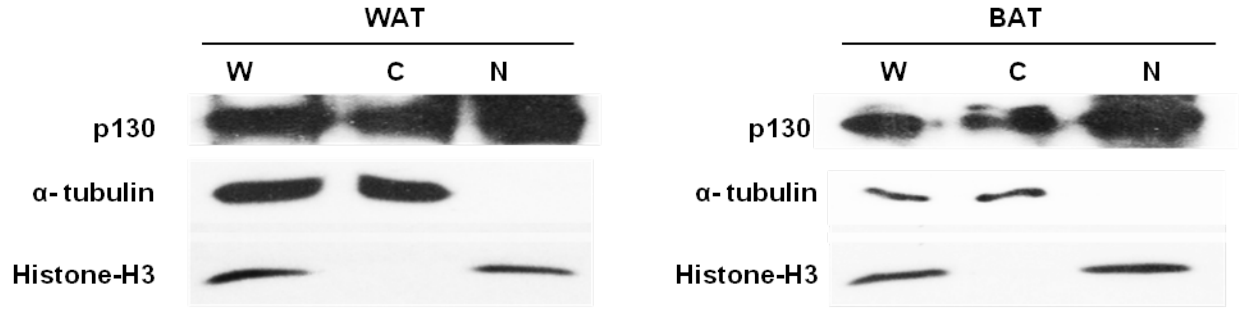

Figure 5. p130 is expressed in white and brown adipose tissues in vivo. (A) Representative Western blot and for p130 and α-tubulin (control) of white adipose tissue (WAT) and brown adipose tissue (BAT) from Balb/c mice. **(B)** Representative Western blot for p130, α-tubulin (cytoplasmic control), and histone H3 (nuclear control) of whole cell (W), cytoplasmic (C) and nuclear (N) fractions from subcutaneous inguinal WAT and interscapular BAT of Balb/c mice.

Figure 6

A

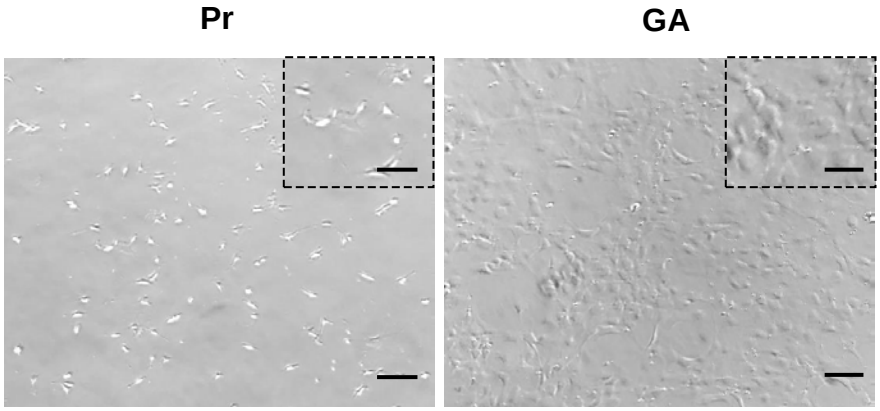

B

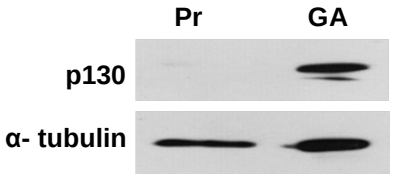

Figure 6. p130 is expressed at growth arrest. (A) Brightfield microscope images for cells above. (Scale bars are equal to 100 μm, and 50 μm in the insets). **(B)** Representative Western blot for p130 and α-tubulin (control) during proliferation (Pr) and growth arrest (GA) in C3H10T1/2 cells.

Figure 7

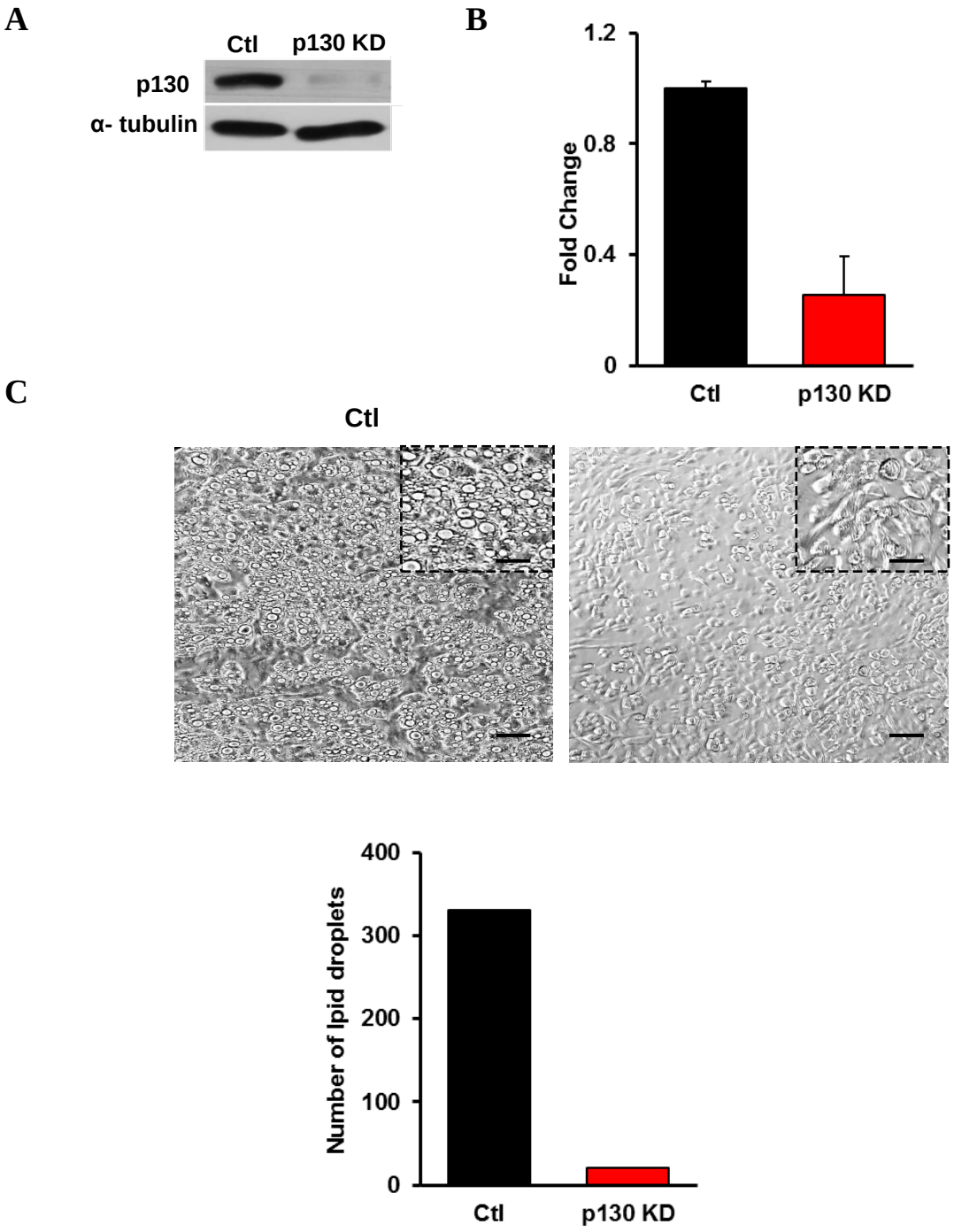

Figure 7. p130 knock down impairs terminal adipocyte differentiation. (A) Representative Western blot for p130 and α-tubulin from control (Ctl) and p130 knock down (KD) C3H10T1/2 cell lines differentiated for 9 days. **(B)** Graphical enumeration for p130 KD C3H10T1/2 differentiated adipocytes (n=2). **(C)** Brightfield microscope images and graphical enumeration of lipids droplets in the microscopic fields of cells above. (Scale bars are equal to 100 μm, and 50 μm in the insets).

Figure 8

A

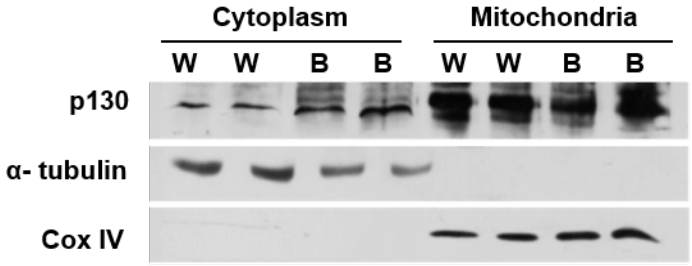

B

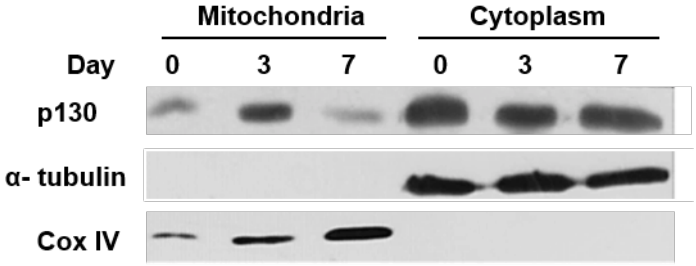

C

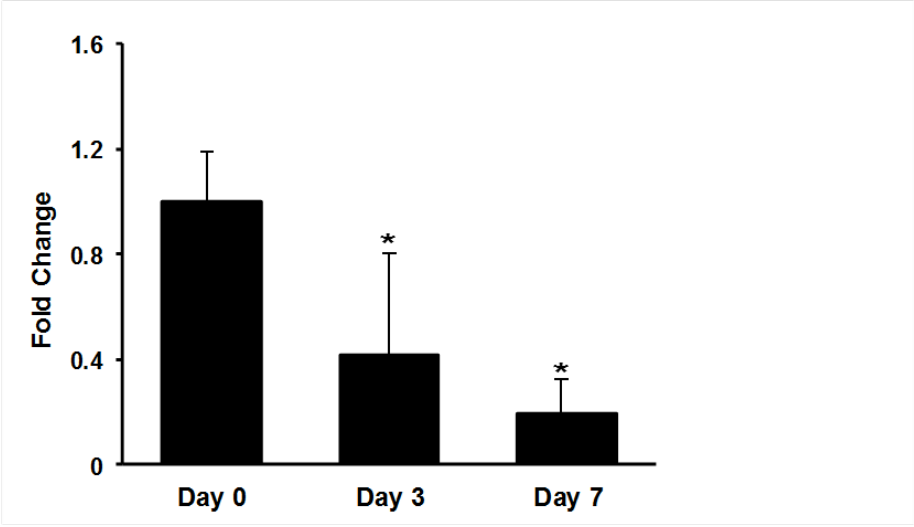

Figure 8. p130 is localized in the mitochondria during adipocyte differentiation and in differentiated adipocytes. (A) Representative Western blot for p130, α-tubulin (cytoplasmic controls) and Cox IV (mitochondrial control) of cytoplasmic and mitochondrial fractions from white (W) and brown (B) adipocytes. (**B**) Representative Western blot of mitochondrial and cytoplasmic fractions for p130, α-tubulin (cytoplasmic control) and Cox IV (mitochondrial control) at days 0, 3 and 7 of C3H10T1/2 adipocyte differentiation. **(C)** Graphical enumeration of mitochondrial protein levels for p130 (n = 3, One-way ANOVA and Tukey post-hoc tests, asterisks denote significance *$p< 0.05$). All data are mean +/- SD.

Figure 9

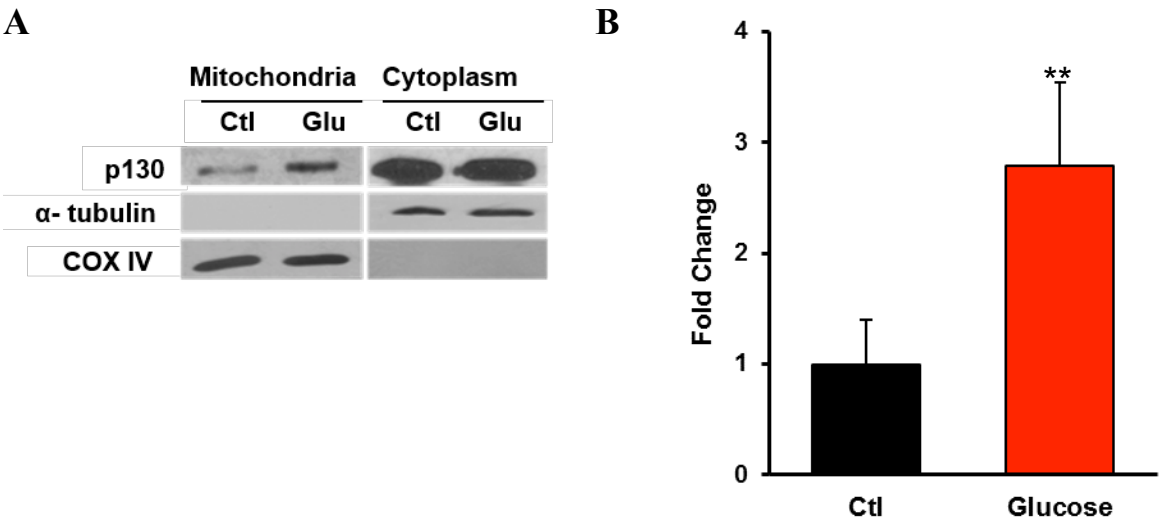

Figure 9. Induction of de novo lipogenesis increases p130 mitochondrial localization in differentiated C3H10T1/2 adipocytes. (A) Representative Western blot of the cytoplasmic and mitochondrial fractions for p130, α-tubulin (cytoplasmic control) and CoxIV (mitochondrial control) in differentiated C3H10T1/2 adipocytes untreated (Ctl) or treated with 100mM glucose (Glu). **(B)** Graphical enumeration of mitochondrial fractions of **(A).** (n = 4, asterisks denote significance $^{**}p < 0.01$).

Figure 10

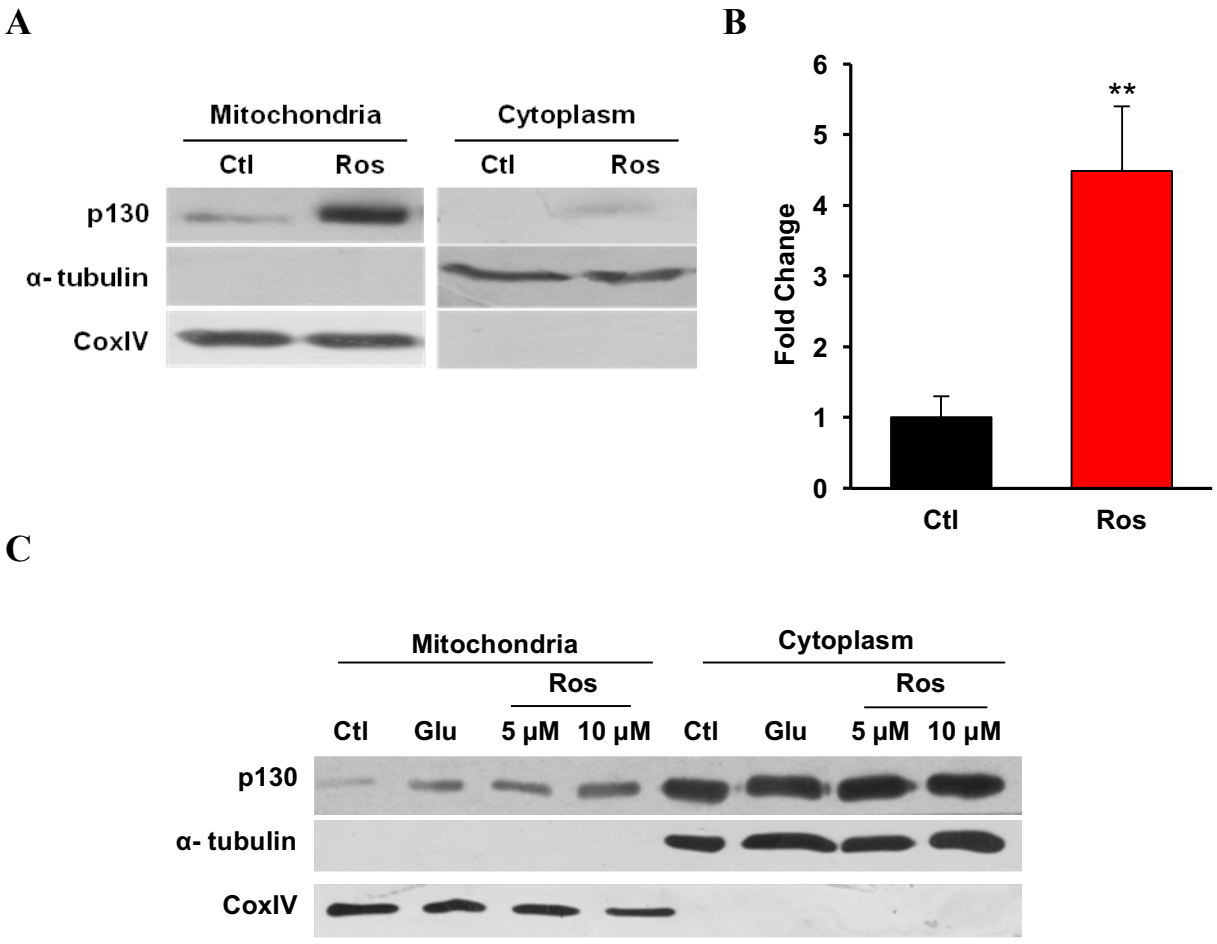

Figure 10. Rosiglitazone increases p130 mitochondrial localization in differentiated C3H10T1/2 adipocytes. (A) Representative Western blot and **(B)** graphical enumeration of the cytoplasmic and mitochondrial fractions for p130, α-tubulin (cytoplasmic control) and CoxIV (mitochondrial control) in differentiated C3H10T1/2 adipocytes untreated or treated with 10μM of rosiglitazone. (n=3, asterisks denote significance $**p < 0.01$). **(C)** Representative Western blot of the cytoplasmic and mitochondrial fractions for p130, α-tubulin (cytoplasmic controls) and CoxIV (mitochondrial control) in differentiated C3H10T1/2 adipocytes untreated (Ctl) or treated with 100mM glucose (Glu), 5μM or 10μM of rosiglitazone (Ros).

Figure 11

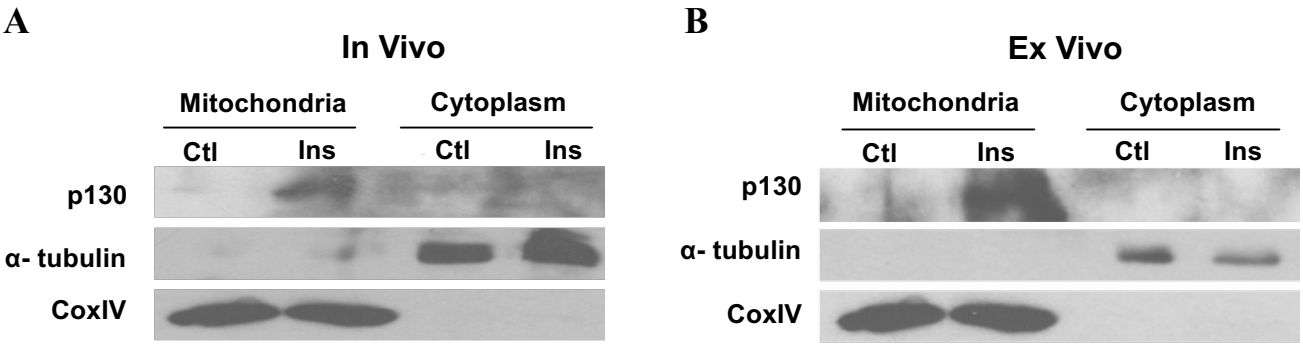

Figure 11. Insulin-induced de novo lipogenesis increases p130 mitochondrial localization in vivo. (A) Representative Western blot of the cytoplasmic and mitochondrial fractions for p130, α-tubulin (cytoplasmic control) and CoxIV (mitochondrial control) in white adipocytes from Balb/c mice injected with saline (Ctl) or insulin (Ins) for 30 minutes. **(B)** Representative Western blot of ex vivo cytoplasmic and mitochondrial fractions for p130, α-tubulin (cytoplasmic control) and CoxIV (mitochondrial control) in white adipocytes untreated and treated with 850 nM insulin for 30 minutes.

Figure 12

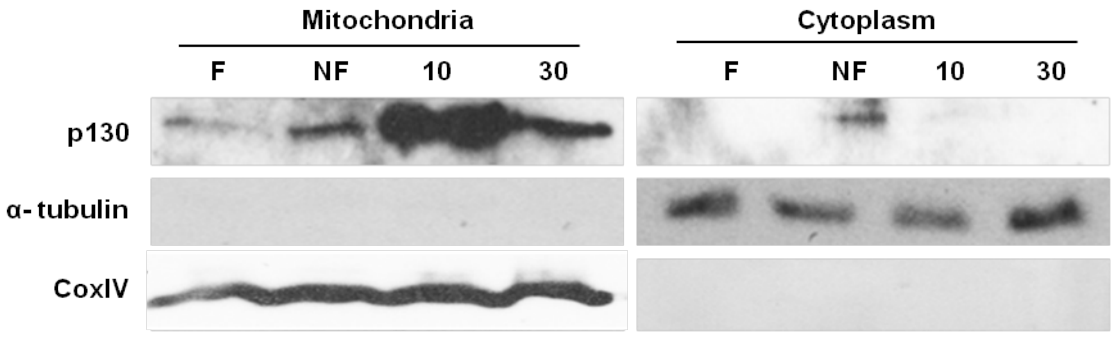

Figure 12. Fasting induces lipolysis decreases p130 levels in primary brown adipocytes. Representative Western blot of the cytoplasmic and mitochondrial fractions for p130, α-tubulin (cytoplasmic control) and Cox IV (mitochondrial control) in primary brown adipocytes from Balb/c mice fasted for 18 hours (F), non-fasted (NF), and injected with 1mg/g glucose for 10 and 30 minutes.

Figure 13

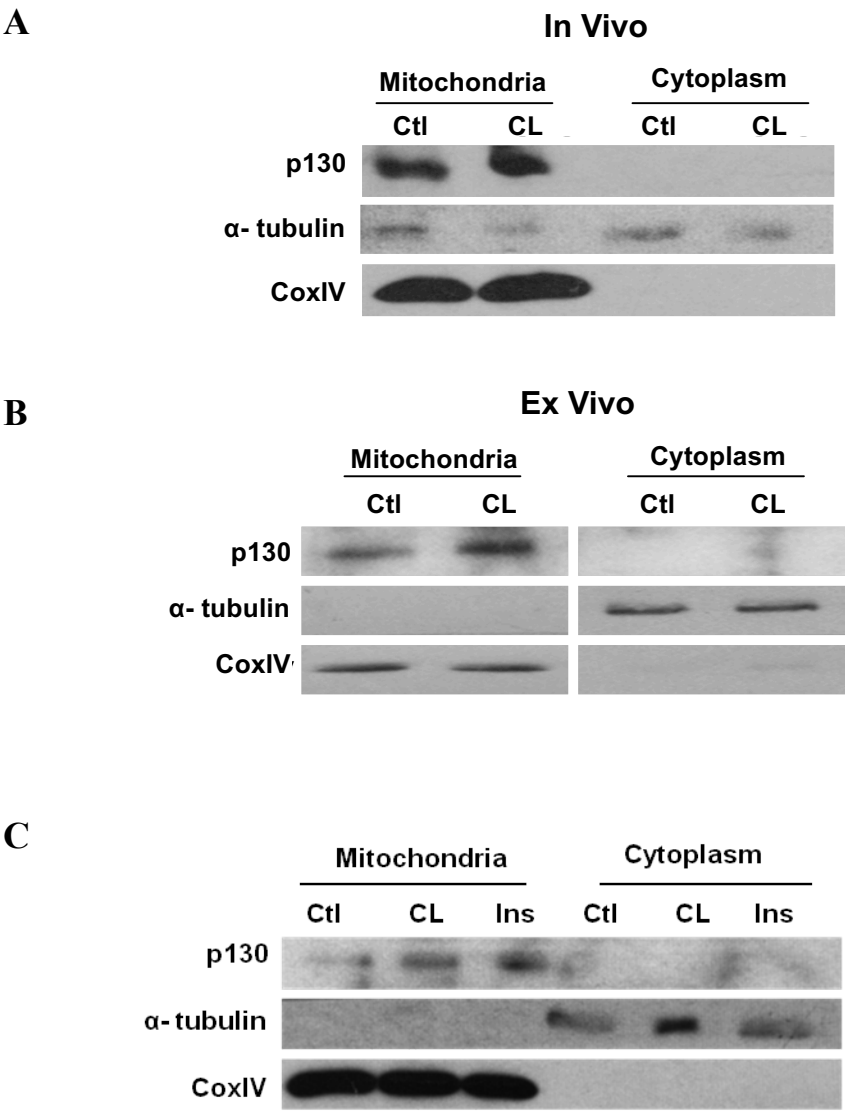

Figure 13. β_3-adrenergic agonist CL, 316 243 increases p130 mitochondrial localization in primary brown adipocytes. **(A)** Representative Western blot of the cytoplasmic and mitochondrial fractions for p130, α-tubulin (cytoplasmic control) and Cox IV (mitochondrial control) in brown adipocytes from Balb/c mice injected with saline (Ctl) or 1mg/kg CL for 5 hours. **(B)** Representative Western blot of ex vivo cytoplasmic and mitochondrial fractions for p130, α-tubulin (cytoplasmic control) and Cox IV (mitochondrial control) in brown adipocytes untreated and treated with 2μM CL for 5 hours. **(C)** Representative Western blot of ex vivo cytoplasmic and mitochondrial fractions for p130, α-tubulin (cytoplasmic control) and Cox IV (mitochondrial control) in brown adipocytes untreated and treated with 40 μM CL for 5 hours and 850 nM insulin for 30 minutes.

Figure 14

A

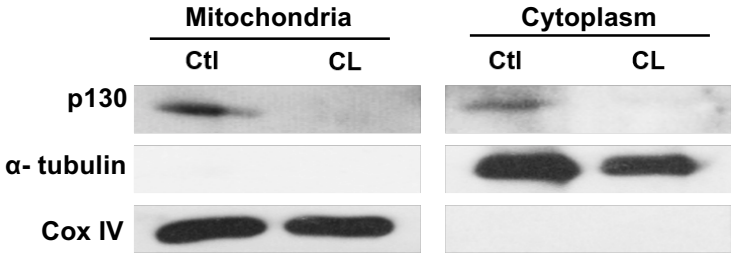

B

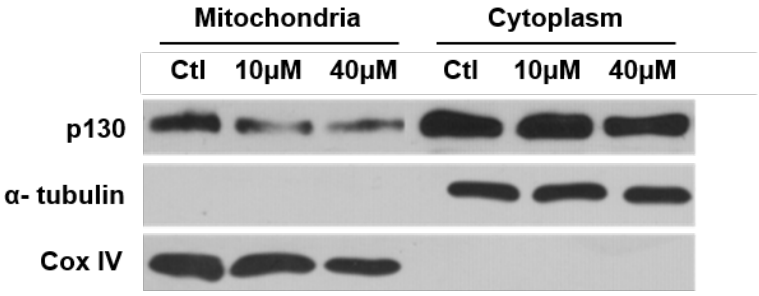

Figure 14. β_3-adrenergic agonist decreases p130 mitochondrial localization in white adipocytes. (A) Representative Western blot of cytoplasmic and mitochondrial fractions for p130, α-tubulin (cytoplasmic control) and Cox IV (mitochondrial control) in white adipocytes from Balb/c mice injected with saline (Ctl) or 1mg/kg CL 316, 243 (CL) for 5 hours. **(B)** Representative Western blot of cytoplasmic and mitochondrial fractions for p130, α-tubulin (cytoplasmic control) and Cox IV (mitochondrial control) in differentiated C3H10T1/2 adipocytes untreated or treated with 10 and 40 μM CL for 5 hours.

Figure 15

A

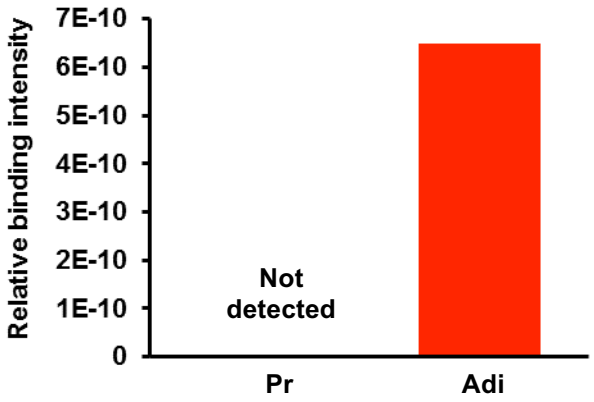

Figure 15. p130 binds at the D-loop regulatory region of mitochondrial DNA. Relative binding intensity of p130 to the D-loop regulatory region in proliferating (Pr) and differentiated C3H10T1/2 adipocytes (Adi). No signal was detected in proliferating cells.

Figure 16

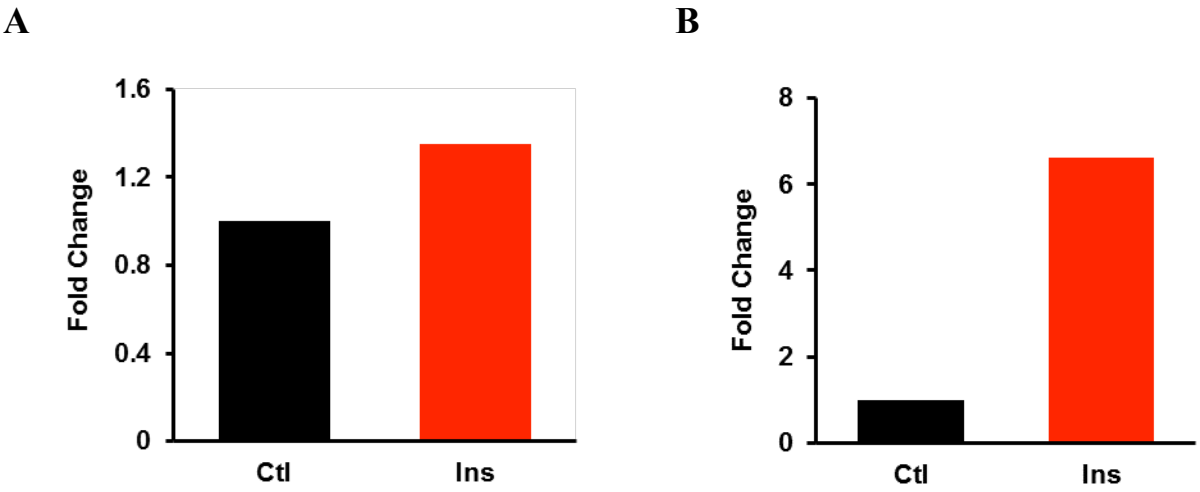

Figure 16. p130 binding at the D-loop regulatory region of mitochondrial DNA increased with insulin treatment. Binding capacity of p130 to the D-loop regulatory region as measured by amplification with D-loop primer sets in (**A**) white and (**B**) brown adipocytes from Balb/c mice that were injected with saline (Ctl) or insulin (Ins) for 30 minutes. Values normalized to Ctl.

Figure 17

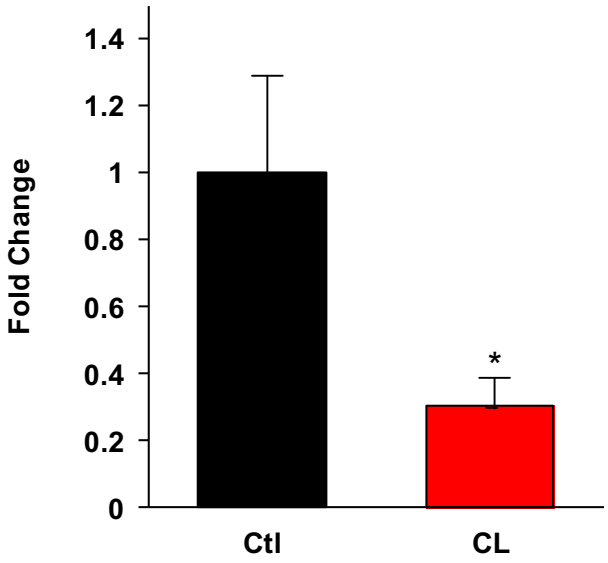

Figure 17. p130 binding at the D-loop regulatory region of mitochondrial DNA is decreased with CL, 316 243 treatment. Binding capacity of p130 as measured by D-loop 1 to the D-loop regulatory region of adipocyte differentiated mouse embryonic fibroblasts untreated (Ctl) or treated with 40 μM CL 316 243 (CL) for 5 hours. (n=3, asterisks denote significance *$p<$ 0.05). Values normalized to Ctl. All data are mean +/- SD.

Figure 18

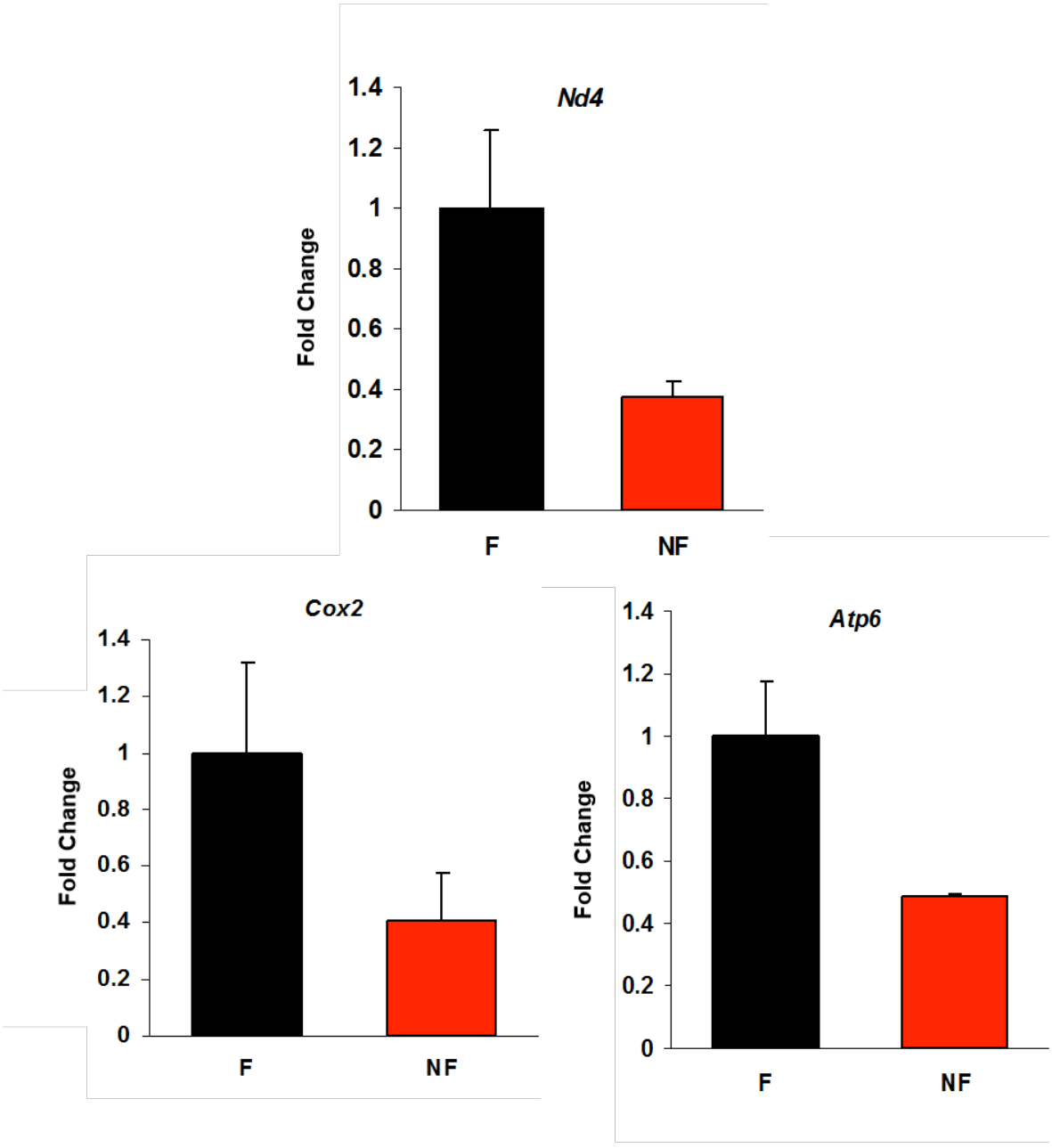

Figure 18. Mitochondrial-encoded OXPHOS genes are upregulated in primary brown adipocytes during lipolysis caused by fasting. Gene expression analysis by qPCR for mitochondrial-encoded OXPHOS genes *Nd4* (Complex 1), *Cox2* (Complex 4) and *Atp6* (Complex 5) of brown adipocytes from fasting (F) and non-fasting (NF) Balb/c mice. (n=2). Values normalized to Ctl. All data are mean +/- SD.

Figure 19

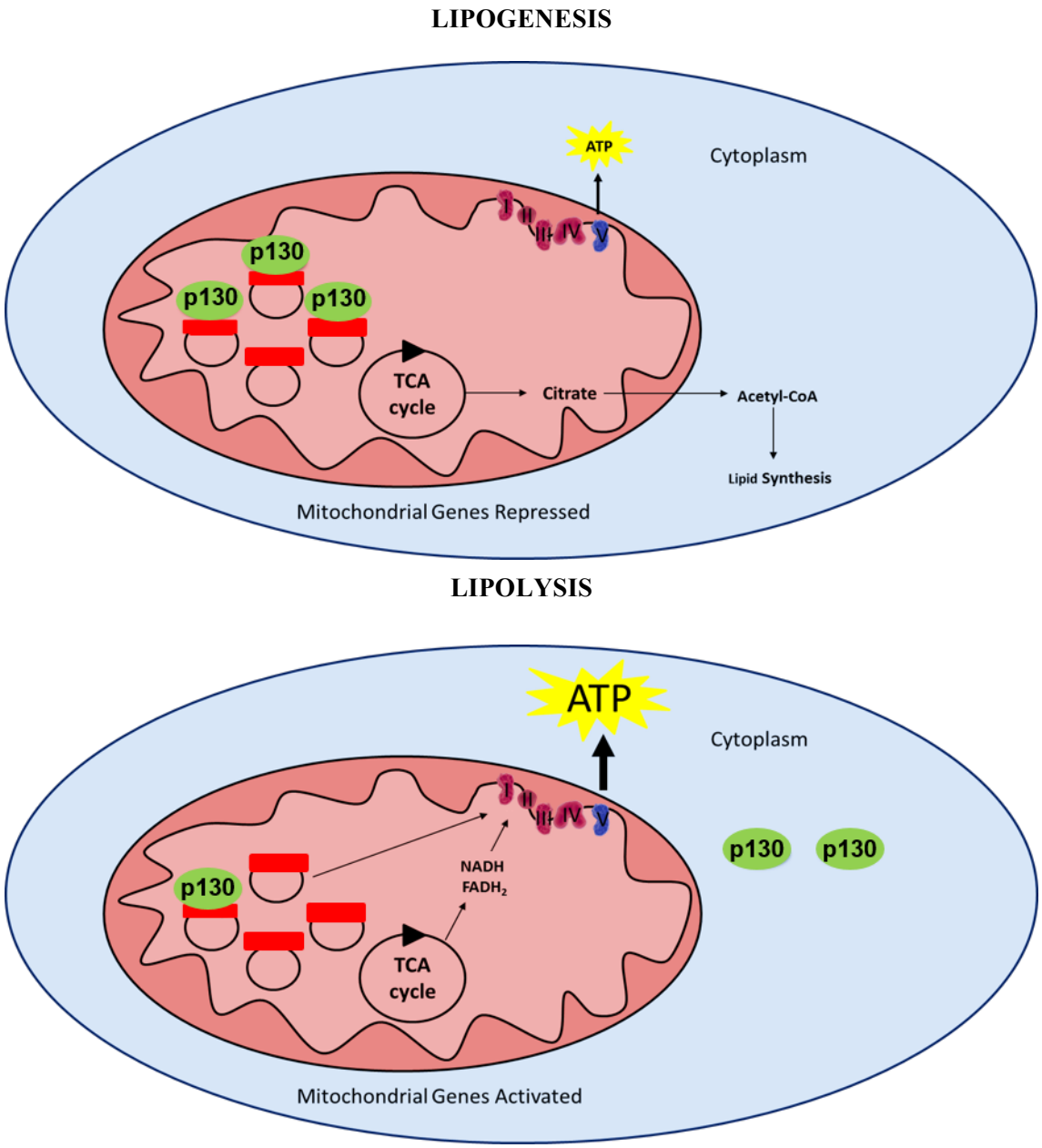

Figure 19. Differential localization of p130 is based on adipocyte cell function. A schematic representation illustrating the metabolic role of p130 in lipogenesis and lipolysis in adipocytes. Nutritional, hormonal or chemical stimuli of lipogenesis result in increased p130 levels in the mitochondria, that interact with the mtDNA promoter at the D-loop region (red) to repress mitochondrial-encoded genes involved in oxidative phosphorylation (complexes I, III, IV, and V). This allows intermediates of the TCA cycle, such as citrate, to be converted into Acetyl-CoA and utilized for lipid synthesis. Conditions activating lipolysis and oxidation of fatty acids and glucose, result in decreased levels of p130 in the mitochondria. This activation of mitochondrial promoters increases the expression of mitochondrial-encoded OXPHOS genes. Abbreviations: TCA, tri carboxylic acid; ATP, Adenosine triphosphate.

5. DISCUSSION

Our study is the first to uncover an unexpected role for the Rb protein family member p130 in potentially regulating fatty acid synthesis and mobilization by controlling mitochondrial gene expression. This data has added another layer of depth and complexity to the dynamism of mitochondrial gene transcription. We show that subcellular localization of p130 is associated with the regulation of fatty acid metabolism in adipocytes. Indeed, stimulating de novo lipogenesis increased p130 levels in the mitochondria where it interacted at the D-loop regulatory region of mitochondrial DNA (mtDNA) to repress genes involved in oxidative phosphorylation (OXPHOS). This would allow TCA cycle intermediates such as citrate to be utilized for lipid synthesis in lieu of energy production (**Fig. 2**). Conversely, inducing lipolysis in white adipocytes via thermogenic activation by β_3-adrenergic signaling decreased p130 levels in the mitochondria. We believe this decrease would prevent citrate from exiting the TCA cycle to make fatty acids. Instead, the TCA cycle would undergo complete turns of oxidation reactions to generate reducing agents such as NADH and $FADH_2$, which are shuttled to the electron transport chain (ETC) for OXPHOS. Intriguingly, adrenergic stimulation in brown adipocytes increased mitochondrial p130 levels. This difference may be linked to the differential regulation and unique molecular composition of brown adipocytes, as they are thermogenic cells expressing Ucp-1. Furthermore, the non-overlapping functions of the different βAR subtypes (β_1, β_2, and β_3ARs) and their ability to couple different signal signaling pathways (Collins and Surwit, 2001; Miniaci et al., 2013) may result in the opposite responses observed between white and brown adipocytes. Together, our data supports a potential novel function of p130 in adipocyte metabolism through governing fatty acid synthesis and mobilization.

The Rb family proteins (Rb, p107/Rbl1, and p130/Rbl2) have been best described according to their nuclear function as molecular corepressors of mammalian cell growth and proliferation (Henley and Dick, 2010; Balciunaite et al., 2005). While Rb is expressed in both proliferating and non-proliferating cells, p130 is most prominently expressed in differentiated or quiescent cells in G_0 (Macaluso et al., 2006). This was confirmed by the expression of p130 at growth arrest and not in proliferating C3H10T1/2 cells during in vitro differentiation (**Fig. 6B**).

The role of p130 during adipocyte differentiation is obscure. Differentiation begins after growth arrest and is thought to be divided into three distinct phases in vitro, which includes an initial commitment step to the adipocyte lineage, followed by mitotic clonal expansion and termination differentiation (Tang et al., 2004). Key features of differentiation include expression of lipogenic proteins, developed sensitivity to hormones such as insulin, and extensive lipid accumulation (Rosen and Spiegelman, 2000). Several studies have investigated the pattern of p130 protein levels across the differentiation of 3T3-L1 preadipocyte cell lines and found that p130 protein levels decrease during differentiation (Fajas et al., 2002; Richon et al., 1997). However, how p130 function in C3H10T1/2 differentiation is not known.

We found that mitochondrial p130 might be required for lipogenesis in early adipocyte differentiation. We show for the first time p130 protein localization in the mitochondria of during C3H10T1/2 cell differentiation into adipocytes. Its levels are highest at growth arrest and decreases over the course of differentiation (**Fig. 8B and 8C**). Notably, a metabolic shift from glycolytic to oxidative metabolism occurs in the early stages of adipocyte differentiation (Drehmer et al., 2016), suggesting a pivotal role for mitochondrial p130 de-repressing OXPHOS capacity. Moreover, the knock down of p130 during differentiation of bone marrow stromal progenitor cells inhibited permanent cell cycle exit and resulted in dysregulated lipid uptake and

release (Capasso et al., 2014). We also found that the reduction of p130 in C3H10T1/2 progenitor cells resulted in impaired terminal differentiation into adipocytes, forming significantly fewer lipid droplets (**Fig. 7**). Thus, p130 may also serve as a surveillance protein for nutrient (fatty acid and glucose) availability during C3H10T1/2 cell differentiation altering OXPHOS by regulating mitochondrial gene expression. Further studies to discern the involvement of p130 in lipogenesis during adipocyte differentiation might make use of p130 deletion mutants that would be incapable of entering the mitochondria.

To our knowledge, we are the first to document a negative correlation between lipogenesis and mitochondrial gene transcription that is mediated by p130 subcellular localization. We demonstrated that certain nutritional and chemical stimuli manipulate p130 mitochondrial localization that might be important to alter the metabolic program of adipocytes. De-novo lipogenesis in humans is known to occur under specific conditions, such as a high fat and/or high carbohydrate intake (Solinas et al., 2015; Saponaro et al., 2015). A study conducted by Collins et al. investigated the induction of de novo lipogenesis in human adipocyte differentiation in vitro by adding exogenous glucose as major precursor (Collins et al., 2011).
We mimicked a carbohydrate-rich environment by adding glucose to C3H10T1/2 differentiated adipocytes. Interestingly, inducing de novo lipogenesis by glucose treatment increased mitochondrial p130 protein levels in these cells (**Fig. 9**). Similarly, treatment with rosiglitazone, a PPAR-γ agonist known to increase glucose uptake and fatty acid esterification into triglycerides (Festuccia et al., 2009), also resulted in increased p130 protein levels in the mitochondria of differentiated C3H10T1/2 cells (**Fig. 10**). Together, this data provides compelling evidence linking the presence of p130 in the mitochondria with lipogenesis in adipocytes.

To ascertain if this new mechanism for lipogenesis has a physiological role, we injected adult mice with insulin for 30 minutes. The downstream target of insulin is mTOR, which subsequently activates SREBP-1c, which induces de novo lipogenic gene expression (Chakrabarti et al., 2010; Laplante and Sabatini, 2009; Porstmann et al., 2008) and also inhibits lipolysis (Gastaldelli, 2011). Insulin tolerance tests of mice fed ad libitum revealed that blood glucose levels dropped 30 minutes post-insulin injection before rising over time (Shao et al., 2012). This suggests that lipogenesis induced by insulin treatment occurs in the short-term. Our results reveal increased p130 localization in the mitochondria of both white and brown adipocytes within 30 minutes (**Fig. 11 and 13C**), increasing the potential for de novo lipogenesis. Increased mitochondrial p130 levels was associated with decreased expression of mitochondrial-encoded OXPHOS genes that would potentially allow TCA cycle intermediates to be utilized for fatty acid synthesis rather than be used to form reducing agents for energy production. In the context of cellular metabolism, the maintenance and expression of mitochondrial genes is important to consider. The mitochondria are very dynamic organelles and the half-life of mitochondrial mRNA encoding OXPHOS proteins is very short (Pearce et al., 2017). Moreover, mitochondrial biogenesis is not necessarily associated with ETC capacity (Rowe et al., 2013), suggesting that the expression of ETC complexes is potentially regulated by p130 and not changes in mitochondrial biogenesis. Hence, hormonal induction of lipogenesis through insulin signaling augments p130 mitochondrial localization similar to the effects of glucose and rosiglitazone in C3H10T1/2 differentiated adipocytes.

To confirm that p130 acts as a lipogenic-inducing factor, measurement of cytoplasmic citrate levels, as well as protein levels or activities of lipogenic enzymes involved in de novo lipogenesis, such as ATP citrate lyase and Acetyl-CoA carboxylase would be required. Increased

citrate levels serves as a marker for increased enzyme kinetics in the de novo lipogenesis pathway, as citrate allosterically activates ACC through a feedforward loop and may directly increase malonyl-CoA concentration (Jewett et al., 2013).

Lipid metabolism is very responsive to changes in the diet (Puca et al., 2008). Physiologically, fasting leads to an increase in the rate of lipolysis while decreasing lipogenesis in adipose tissue, which results in a net loss of triglycerides stored in fat cells (Ahmadian et al., 2007, Vaillancourt et al., 2009). Furthermore, the activation of pathways involved in the transcriptional regulation of de novo lipogenesis are induced by feeding (Kawano & Cohen, 2013; Oosterveer & Schoonjans, 2014). During fasting, adipocytes are known to begin breaking down triglyceride stores through the hydrolytic activity of lipases to supply free fatty acids to other energy demanding tissues such as the brain, liver, and muscle (Gilham and Lehner, 2004; Gibbons et al., 2000). The liver, for instance, utilizes free fatty acids to build triglycerides during fasting (Takeuchi, et al., 2016). We show that mitochondrial p130 localization was attenuated in brown adipocytes from adult mice subjected to an 18h fast (**Fig. 12**). Our results further show that decreased mitochondrial p130 localization in brown adipocytes of fasted mice was associated with increased expression of mitochondrial-encoded OXPHOS genes (**Fig. 18**). Collectively, this data reveals that in fasting conditions or in times of energy deprivation, p130 does not localize in the mitochondria of brown adipocytes, which might help to shift their metabolic focus from building triglycerides to rapidly mobilizing fatty acids for whole body energy homeostasis. In an attempt to reverse the lipolytic state induced in the fasted mice, we injected glucose to mimic a fed state. As expected, mitochondrial p130 levels increased 10 minutes post-injection, which was higher compared to 30-minutes post-injection (**Fig. 12**). This effect was consistent with glucose treatment in differentiated C3H10T1/2 adipocytes. Further

studies will entail investigating how p130 functions in white adipocytes during fasting and/or feeding.

Our results can be placed in the context of metabolic disease such as obesity and Type 2 diabetes. In both conditions, there is dysregulated lipogenesis (Saponaro et al., 2015). In a rodent model of obesity or diabetes, it would be of interest to study how p130 functions in adipocytes and whether mitochondrial gene expression based on p130 subcellular localization could still function. Thus, further experiments will study p130 dynamics, mitochondrial gene expression and lipogenic enzymes in normal, Type 2 diabetic and obese rodents that exhibit insulin resistance and metabolic dysregulation. This will give us a better understanding of the physiological role of p130 in controlling the dynamics of mitochondrial gene expression.

Counterintuitively, we found differences for the way p130 functions in the mitochondria of white and brown fat. Our data shows that while p130 protein expression levels are comparable in both cell types (**Fig. 5**), its subcellular localization is dependent on the type of nutritional, chemical, or hormonal cues. The reason for this is the distinct molecular and functional differences between white and brown adipose tissues in humans and rodents (Chen et al., 2016). White adipocytes located in WAT depots function mainly in triglyceride storage and act as important endocrine cells secreting hormones such as leptin that affects the brain as well as the pancreas, muscles and liver (Paz-Filho et al., 2012; Trayhurn and Beattie, 2001). On the other hand, the primary function of brown and beige adipocytes is to dissipate energy through heat production (Rosell et al., 2014). We used a highly selective β_3-adrenergic agonist, CL 316, 243 (CL) to study p130 function during lipolysis (Klaus et al., 2001). CL treatment is known to decrease lipid accumulation in white adipocytes due to increased lipolytic activity (Klaus et al., 2001). As expected, increasing concentrations of CL attenuated mitochondrial p130 levels in

differentiated C3H10T1/2 adipocytes (**Fig. 14B**). Similar results were obtained in primary white adipocytes from adult mice injected with CL for 5 hours (**Fig. 14A**). However, ex vivo and in vivo brown adipocytes unexpectedly showed increased mitochondrial p130 levels with CL treatment (**Fig. 13**). This difference in the response to CL treatment may emanate from the differential function of brown adipocytes, as they are thermogenic cells expressing Ucp-1. Indeed, chronic CL treatment in brown adipocytes has been previously shown to significantly down-regulate mitochondrial-encoded ATP6 and 8 (part of mitochondrial ATP Synthase, or complex V) (Shore et al., 2013). Increased p130 localization with acute CL treatment in brown adipocytes suggests that it may explicitly repress ATP synthase expression. This could allow the proton gradient to be dissipated mainly through Ucp-1. Moreover, brown adipocytes also contain two other receptors, β_1AR and β_2AR that might influence brown adipocytes differently (Collins and Surwit, 2001).

To date, there are only a limited number of proteins that have been identified to bind to mtDNA. These include Tfam, a positive transcriptional activator of mtDNA transcription, which can bind specifically around the transcription initiation site within the D-loop or non-specifically to other regions of mtDNA (Ngo et al., 2014; Kasashima et al., 2010). Other factors previously characterized as nuclear transcription factors and co factors have also been identified. For example, p53 also been shown to bind to mtDNA and aid in mtDNA repair (Bakhanashvili et al., 2008; Achanta et al., 2005). To increase the complexity of mtDNA transcriptional regulation, p53 can simultaneously repress the activity of nuclear Pgc-1α and repress Pgc-1α -mediated transcription of Tfam (Safdar et al., 2016). In addition, there is recent evidence that STAT3, a member of the STAT protein family that plays a key role in cell growth and pluripotency of stem cells (Takahashi & Yamanaka, 2006; Yang et al, 2010; van Oosten et al, 2012; Martello et al,

2013; Stuart et al, 2014), directly induced transcription of the mitochondrial genome by binding to the D-loop. ChIP-seq results also indicated significant enrichment of Stat3 binding to two regions of the D-loop (Carbognin et al., 2016). Indeed, p130 was found to interact with the D-loop regulatory region as well (**Fig. 15**). Insulin treatment which increased mitochondrial p130 protein levels in vivo showed increased binding in both white and brown tissues (**Fig. 16**), while differentiated mouse embryonic fibroblasts treated with CL showed decreased binding to the D-loop region (**Fig. 17**). Potential p130 binding partners include E2F4/5 or TFAM, however these interactions remain elusive. To confirm that p130 interacts at the D-loop region, future studies will involve the generation of a luciferase reporter construct containing the mouse D-loop DNA followed by a minimal promoter and the open reading frame of the firefly luciferase (Carbognin et al., 2016).

How p130 is shuttled across the mitochondrial membrane remains unresolved. The majority of nuclear-encoded mitochondrial proteins are imported into the mitochondrial matrix by translocator complexes depending on the targeting signal they contain. These are a cleavable N-terminal presequence or a non-cleavable internal targeting sequence (Chacinska, et al., 2009). However, about 30% of mitochondrial proteins lack the N-terminal targeting signals (Diekert et al., 1999). Two software prediction programs, Target P 1.1 (http://www.cbs.dtu.dk/services/TargetP/) and MitoFates (http://mitf.cbrc.jp/MitoFates/cgi-bin/top.cgi), used to identify mitochondrial targeting sequences and cleavage sites confirmed that p130 does not possess a cleavable N-terminal pre sequence (Fukasawa et al., 2015; Emanueolsson et al., 2000; Nielsen et al., 1997). Although both programs indicated a potential cleavage site at amino acid 69, we do not see a truncated or cleaved form of mitochondrial p130. Thus, p130 may contain a non-cleavable internal mitochondrial localization sequence that is not

cleaved after import into the mitochondrial matrix. A potential mechanism for p130 import/export into the mitochondria may involve internal sequence recognition by the Tom70 receptor in the outer mitochondrial membrane, with subsequent translocation across Tom40 to the Tim23 complex that mediates translocation across the inner mitochondrial membrane and into the matrix with the help of Hsp70 (Becker et al., 2012; Dudek et al., 2012; Jensen et al., 2002).

Our current study underscores the potential of mitochondrial-encoded OXPHOS gene regulation that is associated with the metabolic network of the cell. Indeed, our hypothesis has introduced a novel and intriguing role for p130 in the mitochondria of adipocytes regulating its gene transcription, ultimately supporting fatty acid biosynthesis and hydrolysis (**Fig. 19**). Stimulating lipogenesis which increased p130 levels in the mitochondria was associated with increased p130 interaction at the D-loop regulatory region of mitochondrial DNA. This repressed genes involved in OXPHOS, potentially allowing intermediates of the TCA cycle to be utilized for lipid synthesis in lieu of energy production. Conversely, inducing lipolysis in white adipocytes via β_3-adrenergic activation decreased p130 levels in the mitochondria, concomitant with increased mitochondrial-encoded gene expression. Whilst p130 has conventionally been studied as a nuclear co-repressor of transcription, our data strongly supports an alternative perspective to studying the Rb family of proteins, as well as other nuclear proteins. Ultimately, studying the fundamental molecular pathways underlying lipogenesis and lipolysis in adipocytes can provide valuable insight for treating metabolic diseases, such as obesity and Type 2 diabetes, which are responsible for the greatest morbidity and mortality worldwide.

6. LIMITATIONS

Our findings suggest that p130 mitochondrial localization supports fatty acid synthesis and breakdown in terminally differentiated adipocytes. However, additional work is required to establish a direct effect of p130 on mitochondrial gene transcription. For this, we plan to utilize a reporter construct containing the D-loop regulatory region, with which p130 is shown to interact with, fused to the firefly luciferase ORF. Using this construct in transient transfection assays with overexpressed full-length and deletion mutants of p130 will confirm a direct regulatory function for p130 in repressing mitochondrial gene transcription. Measuring luciferase expression in p130 knockout (KO) or knockdown (KD) cells could serve as a control compared to KO/KD cells co-transfected with p130. Cells in the latter experiment should demonstrate decreased reporter activity. Furthermore, chromatin immunoprecipitation followed by whole-genome sequencing (ChIP-seq) will also be employed to measure enrichment of p130 on the D-loop region and on other potential binding sites on the mitochondrial and nuclear genomes. ChIP-seq would also allow us to assess if there are any differences in nuclear binding abilities of p130 under lipogenic and lipolytic conditions, thus confirming a mitochondrial-specific effect.

To discern if p130 is targeted for proteomic degradation in the mitochondria or changing its subcellular localization, modified forms of p130 (GST-tagged) will be used. In this case, p130 covalently coupled to glutathione can be used to track its subcellular localization and negate the possibly of its proteomic degradation via ubiquitination.

Measuring the expressions and/or activities of key lipogenic and lipolytic enzymes will also be important in establishing a supportive function for p130 in these pathways through regulating mitochondrial gene expression. Of interest would be the analysis of hormone sensitive lipase, the rate-limiting enzyme in lipolysis, and the effects of different activators of lipolysis on

its phosphorylation status. Measurements of citrate levels and plasma free fatty acid concentrations can also be used to evaluate fatty acid metabolism. These measurements can also be evaluated in cells genetically-deleted or overexpressing p130, as well as deletion mutants that abrogate its localization and/or binding to mitochondrial DNA.

7. REFERENCES

1. Abraham, T. M., Pedley, A., Massaro, J. M., Hoffman, U., and Fox, C. S. (2015). Association between visceral and subcutaneous adipose depots and incident cardiovascular disease risk factors. Circulation. *132*(17):1639-47.
2. Achanta, G., Sasaki, R., Feng, L., Carew, J.S., Lu, W., Pelicano, H., Keating, M.J. and Huang, P. (2005). Novel role of p53 in maintaining mitochondrial genetic stability through interaction with DNA Pol γ. EMBO J. *24* (19), 3482-3492
3. Ahmadian, M., Duncan, R.E., Jaworski, K., Sarkadi-Nagy, E. and Sul, H.S. (2007). Triacylglycerol metabolism in adipose tissue. Future Lipidol. *2*, 229-237.
4. Algire, C., Medrikova, D., Herzig, S. (2013). White and brown adipose stem cells: from signaling to clinical implications. Biochim Biophys Acta. *1831*, 896–904.
5. Ameer, F., Scandiuzzi, L., Hasnain, S., Kalbacher, H., and Zaidi, N. (2014). De novo lipogenesis in health and disease. Metabolism. *63*(7), 895-902.
6. Anderson, S. Bankier, A.T., Barrell, B.G., De Bruijn, H.L., Coulson, A.R., Drouin, J, Eperson, I.C., Neirlich, D.P., Roe, B.A., Sanger, F., Schreier, P.H., Smith, A.J.H., Staden, R., and Young, I.G. (1981). Sequence and organization of the human mitochondrial genome. Nature. *290*, 457–465.
7. Andrikopoulos, S., Blair, A. R., Deluca, N., Fam, B. C., and Proietto, J. (2008). Evaluating the glucose tolerance test in mice. Am J Physiol Endocrinol Metab, *295*(6), E1323-E1332.
8. Aon, M. A., Bhatt, N., and Cortassa, S. C. (2014). Mitochondrial and cellular mechanisms for managing lipid excess. Front Physiol. *5*, 282.
9. Arner, P., and Langin, D. (2014). Lipolysis in lipid turnover, cancer cachexia, and obesity-induced insulin resistance. Trends Endocrinol Metab. *25*(5), 255-262.

10. Bakhanashvili, M., Grinberg, S., Bonda, E., Simon, A. J., Moshitch-Moshkovitz, S., and Rahav, G. (2008). p53 in mitochondria enhances the accuracy of DNA synthesis. Cell Death Differ. *15*(12), 1865.

11. Balciunaite, E., Spektor, A., Lents, N.H., Cam, H., te Riele, H., Scime, A., Rudnicki, M.A., Young, R. and Dynlacht, B.D., (2005). Pocket protein complexes are recruited to distinct targets in quiescent and proliferating cells. Mol. Cell. Biol. *25*(18), 8166-8178.

12. Barbatelli, G., I. Murano, Lise Madsen, Q. Hao, M. Jimenez, Karsten Kristiansen, J. P. Giacobino, R. De Matteis, and S. Cinti. (2010). The emergence of cold-induced brown adipocytes in mouse white fat depots is determined predominantly by white to brown adipocyte transdifferentiation. Am J Physiol Endocrinol Metab. *298*(6), E1244-E1253.

13. Becker, T., Böttinger, L., and Pfanner, N. (2012). Mitochondrial protein import: from transport pathways to an integrated network. Trends Biochem Sci. *37*(3), 85-91.

14. Beranger, G.E., Karbiener, M., Barquissau, V., Pisani, D.F., Scheideler, M., Langin, D., and Amri, E.Z. (2013). In vitro brown and "brite"/"beige" adipogenesis: human cellular models and molecular aspects. Biochim Biophys Acta. *1831*, 905-14.

15. Bloom, J. D., Dutia, M. D., Johnson, B. D.,Wissner, A., Burns, M. G., Largis, E. E., Dolan,J. A., and Claus, T. H. (1992). Disodium (R,R)-5-[2-[[2-(3-chlorophenyl)-2-hydroxyethyl]-amino] propyl]-1,3-benzodioxole-2,2-dicarboxylate (CL 316,243). A potent beta-adrenergic agonist virtually specific for beta 3 receptors. A promising antidiabetic and antiobesity agent. J. Med. Chem. *35*, 3081-3084.

16. Boudina, S. and Graham, T. (2014). Mitochondrial function/dysfunction in white adipose tissue. Exp Physiol. *99*, 1168-1178Bartelt, A, and Heeren, J. (2014). Adipose tissue browning and metabolic health. Nat Rev Endocrinol. *10*, 24e36.
17. Brasaemle, D. L., Levin, D. M., Adler-Wailes, D. C., and Londos, C. (2000). The lipolytic stimulation of 3T3-L1 adipocytes promotes the translocation of hormone-sensitive lipase to the surfaces of lipid storage droplets. Biochim. Biophys. Acta, Mol. Cell. Biol. Lipids. *1483*(2), 251-262.
18. Bustin, S.A., Benes, V., Garson, J.A., Hellemans, J., Huggett, J., Kubista, M., Mueller, R., Nolan, T., Pfaffl, M.W., Shipley, G.L. and Vandesompele, J. (2009). The MIQE guidelines: minimum information for publication of quantitative real-time PCR experiments. Clin Chem. *55*(4), 611-622.
19. Cao, W., Medvedev, A. V., Daniel, K. W., and Collins, S. (2001). β-adrenergic activation of p38 MAP kinase in adipocytes cAMP induction of the uncoupling protein 1 (UCP1) gene requires p38 map kinase. J Biol Chem. *276*(29), 27077-27082.
20. Cannon, B. and Nedergaard, J. (2004). Brown adipose tissue: function and physiological significance. Physiol Rev. *84*, 277–359.
21. Capasso, S., Alessio, N., Di Bernardo, G., Cipollaro, M., Melone, M., Peluso, G., Giordano, A. and Galderisi, U. (2014). Silencing of RB1 and RB2/P130 during adipogenesis of bone marrow stromal cells results in dysregulated differentiation. Cell cycle. *13*(3), 482-490.
22. Caputi, M., Russo, G., Esposito, V., Mancini, A., and Giordano, A. (2005). Role of cell-cycle regulators in lung cancer. J Cell Physiol. *205*(3), 319-327.
23. Cederquist, C.T., Lentucci, C., Martinez-Calejman, C., Hayashi, V., Orofino, J., Guertin, D., Fried, S.K., Lee, M.J., Cardamone, M.D. and Perissi, V. (2017). Systemic insulin sensitivity is

regulated by GPS2 inhibition of AKT ubiquitination and activation in adipose tissue. Mol Metab. *6*(1), 125-137.

24. Cedikova, M., Kripnerova, M., Dvorakova, J., Pitule, P., Grundmanova, M., Babuska, V., Mullerova, D., and Kuncova, J. (2016). Mitochondria in White, Brown, and Beige Adipocytes. Stem Cells Int. *2016*, 6067349.
25. Chacinska, A., Koehler, C. M., Milenkovic, D., Lithgow, T., and Pfanner, N. (2009). Importing mitochondrial proteins: machineries and mechanisms. *Cell*, *138*(4), 628-644.
26. Chakrabarti, P., English, T., Shi, J., Smas, C. M., and Kandror, K. V. (2010). Mammalian target of rapamycin complex 1 suppresses lipolysis, stimulates lipogenesis, and promotes fat storage. Diabetes. *59*(4), 775-781.
27. Chandel, N. S. (2014). Mitochondria as signaling organelles. BMC Biol. *12*(1), 34.
28. Chang, J. S., and Ha, K. (2017). An unexpected role for the transcriptional coactivator isoform NT-PGC-1α in the regulation of mitochondrial respiration in brown adipocytes. J Biol Chem. *292*(24), 9958-9966.
29. Chen, Y., Pan, R., and Pfeifer, A. (2016). Fat tissues, the brite and the dark sides. Pflugers Arch. *468*, 1803-1807.
30. Chow, K.N., and Dean, D.C. (1996). Domains A and B in the Rb pocket interact to form a transcriptional repressor motif. Mol Cell Biol. *16*, 4862-4868.
31. Chow, K.B., Starostik, P., and Dean, D.C. (1996). The Rb family contains a conserved cyclin-dependent-kinase-regulated transcriptional repressor motif. Mol Cell Biol. *16*, 7173-7181.
32. Chusyd, D.E., Wang, D., Huffman, D., and Nagy, T.R. (2016). Relationships between rodent white adipose fat pads and human white adipose fat depots. Front Nutr. *3*, 10.

33. Cinti, S., Montana, G., Parker, M.G., and Christian, M. (2014). Brown and white adipose tissues: intrinsic differences in gene expression and response to cold exposure in mice. Am J Physiol Endrocrinol Metabol. *306*, E945-E964.
34. Classon, M. and Dyson, N. (2001). p107 and p130: versatile proteins with interesting pockets. Exp Cell Res. *264*, 135-147.
35. Claudio, P. P., Tonini, T., and Giordano, A. (2002). The retinoblastoma family: twins or distant cousins?. Genome Biol. *3*(9), reviews3012-1.
36. Clifford, G. M., Londos, C., Kraemer, F. B., Vernon, R. G., and Yeaman, S. J. (2000). Translocation of hormone-sensitive lipase and perilipin upon lipolytic stimulation of rat adipocytes. J Biol Chem. *275*(7), 5011-5015.
37. Cobrinik, D. (2005). Pocket proteins and cell cycle control. Oncogene. *24*(17), 2796.
38. Cole, S. W., & Sood, A. K. (2012). Molecular pathways: beta-adrenergic signaling in cancer. Clin. Cancer Res. *18*(5), 1201-1206
39. Collins, J.M., Neville, M.J., Pinnick, K.E., Hodson, L., Ruyter, B., van Dijk, T.H., Reijngoud, D.J., Fielding, M.D. and Frayn, K.N., (2011). De novo lipogenesis in the differentiating human adipocyte can provide all fatty acids necessary for maturation. J. Lipid. R. *52*(9), 1683-1692.
40. Collins, S. and Surwit, R.S. (1996). Pharmacologic manipulation of ob expression in a dietary model of obesity. J Biol Chem. *16*, 9437-40.
41. Collins, S., and Surwit, R. S. (2001). The beta-adrenergic receptors and the control of adipose tissue metabolism and thermogenesis. Recent Prog Horm Res. *56*, 309-328.

42. Cooney, G.J. and Newsholme, E.A. (1982). The maximum capacity of glycolysis in brown adipose tissue and its relationship to control of the blood glucose concentration. FEBS Lett. *148*, 198–200.

43. Costa, J. V., and Duarte, J. S. (2006). Adipose tissue and adipokines. Acta Med Port. *19*(3), 251-6.

44. Crichton, P.G., Lee, Y., and Kunji, E.R.S. (2017). The molecular features of uncoupling protein 1 support a conventional mitochondrial carrier-like mechanism. *134*, 35-50.

45. Crunkhorn, S., and Patti, M. E. (2008). Links between thyroid hormone action, oxidative metabolism, and diabetes risk?. Thyroid. *18*(2), 227-237.

46. Daikoku, T., Shinohara, Y., Shima, A., Yamazaki, N., and Terada, H. (2000). Specific elevation of transcript levels of particular protein subtypes induced in brown adipose tissue by cold exposure. Biochem Biophys Acta. *1457*, 263–272.

47. Davies, R.W., Lau, P., Naing, T., Nikpay, M., Doelle, H., Harper, M.E., Dent, R. and McPherson, R. (2013). A 680 kb duplication at the FTO locus in a kindred with obesity and a distinct body fat distribution. Eur J Hum Genet. *21*(12), 1417.

48. Day, F. R., and Loos, R. J. (2011). Developments in obesity genetics in the era of genome-wide association studies. J Nutrigenet Nutrigenomics. *4*(4), 222-238.

49. de Jong, J. M., Wouters, R. T., Boulet, N., Cannon, B., Nedergaard, J., and Petrovic, N. (2017). The β 3-adrenergic receptor is dispensable for browning of adipose tissues. Am J Physiol Endocrinol Metab. *312*(6), E508-E518.

50. De Pauw, A., Tejerina, S., Raes, M., Keijer, J., and Arnould, T. (2009). Mitochondrial (dys)function in adipocyte (de)differentiation and systemic metabolic alterations. Am J Pathol. *175*, 927-939.

51. De Sousa, M., Porras, D.P., Perry, C.G.R., Seale, P., and Scimè, A. (2014). p107 Is a Crucial Regulator for Determining the Adipocyte Lineage Fate Choices of Stem Cells. Stem Cells. *32*, 1323–1336.

52. Diekert, K., Kispal, G., Guiard, B., and Lill, R. (1999). An internal targeting signal directing proteins into the mitochondrial intermembrane space. Proc. Natl. Acad. Sci., *96*(21), 11752-11757.

53. Drehmer, D.L., Melo de Aguiar, A., Brandt, A.P., Petiz, L., Cadena, S.M.S.C., Rebelatto, C.K., Brofman, P.R.S., Neto, F.F., Dallagiovanna, B., and Abud, A.P.R. (2016). Metabolic switches during the first steps of adipogenic stem cells differentiation. Stem Cell Res. *17*, 413-421.

54. Duffaut, C., Bour, S., Prévot, D., Marti, L., Testar, X., Zorzano, A., and Carpéné, C. (2006). Prolonged treatment with the β3-adrenergic ago-nist CL 316243 induces adipose tissue remodelingin rat but not in guinea pig: 2) modulation of glucose uptake and monoamine oxidase activity. J. Physiol. Biochem. *62*, 101-112.

55. Dudek, J., Rehling, P., and van der Laan, M. (2013). Mitochondrial protein import: common principles and physiological networks. Biochimica et biophysica acta, *1833*(2), 274-285.

56. Duncan, R. E., Ahmadian, M., Jaworski, K., Sarkadi-Nagy, E., and Sul, H. S. (2007). Regulation of lipolysis in adipocytes. Annu Rev Nutr. *27*, 79-101.

57. Egan, J. J., Greenberg, A. S., Chang, M. K., and Londos, C. (1990). Control of endogenous phosphorylation of the major cAMP-dependent protein kinase substrate in adipocytes by insulin and beta-adrenergic stimulation. J Biol Chem. *265*(31), 18769-18775.

58. Egan, J. J., Greenberg, A. S., Chang, M. K., Wek, S. A., Moos, M. C., and Londos, C. (1992). Mechanism of hormone-stimulated lipolysis in adipocytes: translocation of hormone-sensitive lipase to the lipid storage droplet. Proc. Natl. Acad. Sci. U.S.A. *89*(18), 8537-8541.

59. Emanuelsson, O., Nielsen, H., Brunak, S., and Von Heijne, G. (2000). Predicting subcellular localization of proteins based on their N-terminal amino acid sequence. J. Mol. Biol. *300*(4), 1005-1016.

60. Fajas, L., Landsberg, R. L., Huss-Garcia, Y., Sardet, C., Lees, J. A., and Auwerx, J. (2002). E2Fs regulate adipocyte differentiation. Dev. Cell. *3*(1), 39-49.

61. Fedorenko, A., Lishko, P.V., and Kirichok, Y. (2012). Mechanism of fatty-acid-dependent UCP1 uncoupling in brown fat mitochondria. Cell. *151,* 400–13.

62. Fenzl, A., and Kiefer, F.W. (2014). Brown adipose tissue and thermogenesis. Horm Mol Biol Clin Investig. *19*, 25e37.

63. Fernandez-Marcos, P. J., and Auwerx, J. (2011). Regulation of PGC-1α, a nodal regulator of mitochondrial biogenesis. Am J Clin Nutr. *93*(4), 884S-890S.

64. Ferre, P.and F. Foufelle (2007). SREBP-1c Transcription Factor and Lipid Homeostasis: Clinical Perspective. Horm Res. *68*, 72–82.

65. Festuccia, W. T., Blanchard, P.G., Turcotte, V., Laplante, M., Sariahmetoglu, M., Brindley, D.N., and Deshaies, Y. (2009). Depot-specific effects of the PPARg-agonist rosiglitazone on adi-pose tissue glucose uptake and metabolism. J. Lipid Res. *50*, 1185–1194.

66. Festuccia, W.T., Blanchard, P.G., Turcotte, V., Laplante, M., Sariahmetoglu, M., Brindley, D.N., Richard, D. and Deshaies, Y. (2009). The PPARγ agonist rosiglitazone enhances rat brown adipose tissue lipogenesis from glucose without altering glucose uptake. Am J Physiol Regul Integr Comp Physiol. *296*(5), R1327-R1335.

67. Folmes, C. D., Dzeja, P. P., Nelson, T. J., and Terzic, A. (2012). Metabolic plasticity in stem cell homeostasis and differentiation. Cell stem cell. *11*(5), 596-606.

68. Forner, F., Kumar, C., Luber, C.A., Fromme, T., Klingenspor, M., and Mann, M. (2009). Proteome differences between brown and white fat mitochondria reveal specialized metabolic functions. Cell Metab. *10*, 324-35.

69. Frayling, T.M., Timpson, N.J., Weedon, M.N., Zeggini, E., Freathy, R.M., Lindgren, C.M., Perry, J.R., Elliott, K.S., Lango, H., Rayner, N.W. and Shields, B. (2007). A common variant in the FTO gene is associated with body mass index and predisposes to childhood and adult obesity. Science. *316*(5826), 889-894.

70. Fredrikson, G., Strålfors, P., Nilsson, N. O., and Belfrage, P. (1981). Hormone-sensitive lipase of rat adipose tissue. Purification and some properties. J Biol Chem. *256*(12), 6311-6320.

71. Fukasawa, Y., Tsuji, J., Fu, S. C., Tomii, K., Horton, P., and Imai, K. (2015). MitoFates: improved prediction of mitochondrial targeting sequences and their cleavage sites. Mol Cell Proteomics. *14*(4), 1113-1126.

72. Gastaldelli, A. (2011). Role of beta-cell dysfunction, ectopic fat accumulation and insulin resistance in the pathogenesis of type 2 diabetes mellitus. Diabetes Res Clin Pract. *93*, S60-S65.

73. Genovese, C., Trani, D., Caputi, M., and Claudio, P.P. (2006). Cell cycle control and beyond: emerging roles for the retinoblastoma gene family. Oncogene. *25*, 5201-5209.

74. Gesta, S., Tseng, Y.H., and Kahn, C.R. (2007). Developmental origin of fat: tracking obesity to its source. Cell. *131*, 242–256.

75. Ghorbani, M., Teimourian, S., Farzad, R., and Asl, N. N. (2015). Apparent histological changes of adipocytes after treatment with CL 316,243, a β-3-adrenergic receptor agonist. Drug Des. Dev. Ther. *9*, 669.

76. Gibbons, G. F., Islam, K., and Pease, R. J. (2000). Mobilisation of triacylglycerol stores. Biochim. Biophys. Acta, *1483*(1), 37-57.

77. Gilham, D., and Lehner, R. (2004). The physiological role of triacylglycerol hydrolase in lipid metabolism. Rev Endocr Metab Disord. *5*(4), 303-309.

78. Gray, M.W. (1999). Mitochondrial evolution. Science. *283*, 1476-1481.

79. Gray, M.W. (2012). Mitochondrial evolution. Cold Spring Harb Perspect Biol. *4*, a011403.

80. Greenberg, A. S., Egan, J. J., Wek, S. A., Garty, N. B., Blanchette-Mackie, E. J., and Londos, C. (1991). Perilipin, a major hormonally regulated adipocyte-specific phosphoprotein associated with the periphery of lipid storage droplets. J Biol Chem. *266*(17), 11341-11346.

81. Greenberg, A. S., Shen, W. J., Muliro, K., Patel, S., Souza, S. C., Roth, R. A., and Kraemer, F. B. (2001). Stimulation of lipolysis and hormone-sensitive lipase via the extracellular signal-regulated kinase pathway. J Biol Chem. *276*(48), 45456-45461.

82. Gregoire, F.M., Smas, C.M., and Sul, H.S. (1998). Understanding adipocyte differentiation. Physiol. Rev. *78*, 783–809.

83. Grzybowska-Szatkowska, L., Ślaska, B., Rzymowska, J., Brzozowska, A., and Floriańczyk, B. (2014). Novel mitochondrial mutations in the *ATP6* and *ATP8* genes in patients with breast cancer. Mol Med Rep. *10*, 1772–1778.

84. Gustafson, B., and Smith, U. (2015). Regulation of white adipogenesis and its relation to ectopic fat accumulation and cardiovascular risk. Atherosclerosis. *241*(1), 27-35.

85. Harms, M. and Seale, P. (2013). Brown and beige fat: development, function and therapeutic potential. Nat Med. *19*, 1252–1263.

86. Harms, M., and Seale, P. (2013). Brown and beige fat: development, function and therapeutic potential. Nat Med. *19*(10), 1252-1263.

87. Henley, S. A., and Dick, F. A. (2012). The retinoblastoma family of proteins and their regulatory functions in the mammalian cell division cycle. Cell Div. *7*(1), 10.

88. Himms-Hagen, J. and Ghorbani, M. (1998). Treatment with CL 316,243, a beta 3-adrenoceptor agonist, reduces serum leptin in rats with diet- or aging-associated obesity, but not in Zucker rats with genetic (fa/fa) obesity. Int J Obes Relat Metab Disord. *22*, 63-5.

89. Holloway, G. P., Bonen, A., and Spriet, L. L. (2009). Regulation of skeletal muscle mitochondrial fatty acid metabolism in lean and obese individuals. Am J Clin Nutr. *89*(1), 455S-462S.

90. Jensen, R. E., and Dunn, C. D. (2002). Protein import into and across the mitochondrial inner membrane: role of the TIM23 and TIM22 translocons. Biochim. Biophys. Acta. *1592*(1), 25-34.

91. Jewett, M. C., Workman, C. T., Nookaew, I., Pizarro, F. A., Agosin, E., Hellgren, L. I., and Nielsen, J. (2013). Mapping condition-dependent regulation of lipid metabolism in Saccharomyces cerevisiae. G3. *3*(11), 1979-1995.

92. Jimenez, M., Barbatelli, G., Allevi, R., Cinti, S., Seydoux, J., Giacobino, J.P., Muzzin, P. and Preitner, F. (2003). β3-Adrenoceptor knockout in C57BL/6J mice depresses the occurrence of brown adipocytes in white fat. FEBS J. *270*(4), 699-705.

93. Jornayvaz, F. R., and Shulman, G. I. (2010). Regulation of mitochondrial biogenesis. Essays Biochem. *47*, 69-84.

94. Jowett, J.B., Curran, J.E., Johnson, M.P., Carless, M.A., Göring, H.H., Dyer, T.D., Cole, S.A., Comuzzie, A.G., MacCluer, J.W., Moses, E.K. and Blangero, J. (2010). Genetic variation at the FTO locus influences RBL2 gene expression. Diabetes. *59*(3), 726-732.

95. Kajimoto, K., Daikoku, T., Kita, F., Yamazaki, N., Kataoka, M., Baba, Y., Terada, H. and Shinohara, Y. (2003). PCR-select subtraction for characterization of messages differentially expressed in brown compared with white adipose tissue. Mol Genet Metab. *80*, 255–261.

96. Kajimura, S. and Saito, M. (2014). A New Era in Brown Adipose Tissue Biology: Molecular Control of Brown Fat Development and Energy Homeostasis. Annu Rev Physiol. *76*, 225–249.

97. Kajimura, S., Spiegelman, B.M., and Seale, P. (2015). Brown and beige fat: physiological roles beyond heat generation. Cell metab. *22*, 546e59.

98. Kasashima, K., Sumitani, M., and Endo, H. (2011). Human mitochondrial transcription factor A is required for the segregation of mitochondrial DNA in cultured cells. Exp. Cell. Res. *317*(2), 210-220

99. Kersten, S. (2001). Mechanisms of nutritional and hormonal regulation of lipogenesis. EMBO Rep. *2*(4), 282-286.

100. Kersten, S., Seydoux, J., Peters, J. M., Gonzalez, F. J., Desvergne, B., and Wahli, W. (1999). Peroxisome proliferator–activated receptor α mediates the adaptive response to fasting. J Clin Invest. *103*(11), 1489.

101. Kim, E. Y., Kim, W. K., Oh, K. J., Han, B. S., Lee, S. C., and Bae, K. H. (2015). Recent advances in proteomic studies of adipose tissues and adipocytes. Int J Mol Sci., *16*(3), 4581-4599.

102. Klaus, S., Seivert, A., and Boeuf, S. (2001). Effect of the β_3-adrenergic agonist Cl316,243 on functional differentiation of white and brown adipocytes in primary cell culture. Biochimica et Biophysica Acta. *1539*, 85-92.

103. Koh, E.H., Park, J.Y., Park, H.S., Jeon, M.J., Ryu, J.W., Kim, M., Kim, S.Y., Kim, .S., Kim, S.W., Park, I.S., Youn, J.H., and Lee, K.U. (2007). Essential role of mitochondrial function in adiponectin synthesis in adipocytes. Diabetes. *56*, 2973-81.

104. Krentz, A.J and Bailey, C.J. (2005). Oral antidiabetic agents: current role in type 2 diabetes mellitus. Drugs. *65*, 385-41.

105. Kruse, B., Narasimhan, N., and Attardi, G. (1989). Termination of transcription in human mitochondria: identification and purification of a DNA binding protein factor that promotes termination. Cell. *58*(2), 391-397.

106. Laplante, M., and Sabatini, D. M. (2009). An emerging role of mTOR in lipid biosynthesis. Curr Biol, *19*(22), R1046-R1052.

107. Lazar, M.A. (2008). Developmental biology. How now, brown fat? Science. *321,* 1048–1049.

108. Lecoultre, V., and Ravussin, E. (2011). Brown adipose tissue and aging. Curr Opin Clin Nutr Metab Care. *14*(1), 1-6.

109. Leigh-Brown, S., Enriquez, J.A., and Odom, D.T. (2010). Nuclear transcription factors in mammalian mitochondria. Genome Biol. *11*, 215.

110. Litovchick, L., Chestukhin, A., and DeCaprio, J.A. (2004). Glycogen synthase kinase 3 phosphorylates RBL2/p130 during quiescence. Mol Cell Biol. *24*: 8970–8980.

111. Loos, R. J., and Yeo, G. S. (2014). The bigger picture of FTO [mdash] the first GWAS-identified obesity gene. Nat. Rev. Endocrinol. *10*(1), 51-61.

112. Lu, Y., and Loos, R. J. (2013). Obesity genomics: assessing the transferability of susceptibility loci across diverse populations. Genome Med. *5*(6), 55.

113. Macaluso, M., Montanari, M., and Giordano, A. (2006). Rb family proteins as modulators of gene expression and new aspects regarding the interaction with chromatin remodeling enzymes. Oncogene. *25*(38), 5263-5267.

114. Martin, M., Cho, J., Cesare, A.J., Griffith, J.D., and Attardi, G. (2005). Termination factor-mediated DNA loop between termination and initiation sites drives mitochondrial rRNA synthesis. Cell. *123*, 1227–1240.

115. Matsuzawa, Y. (2006). The metabolic syndrome and adipocytokines. FEBS Lett. *580*(12), 2917-2921.

116. Mattsson, C.L., Csikasz, R.I., Chernogubova, E., Yamamoto, D.L., Hogberg, H.T., Amri, E.Z., Hutchinson, D.S. and Bengtsson, T. (2011). β 1-Adrenergic receptors increase UCP1 in human MADS brown adipocytes and rescue cold-acclimated β 3-adrenergic receptor-knockout mice via nonshivering thermogenesis. Am J Physiol Endocrinol Metab. *301*(6), E1108-E1118.

117. Miniaci, M. C., Bucci, M., Santamaria, R., Irace, C., Cantalupo, A., Cirino, G., and Scotto, P. (2013). CL316, 243, a selective β3-adrenoceptor agonist, activates protein translation through mTOR/p70S6K signaling pathway in rat skeletal muscle cells. Pflugers Arch., EJP. *465*(4), 509-516.

118. Mottillo, E. P., Balasubramanian, P., Lee, Y. H., Weng, C., Kershaw, E. E., and Granneman, J. G. (2014). Coupling of lipolysis and de novo lipogenesis in brown, beige, and white adipose tissues during chronic β3-adrenergic receptor activation. J Lipid Res., *55*(11), 2276-2286.

119. Mouchiroud, L., Eichner, L.J., Shaw, R., and Auwerx, J. (2014). Transcriptional coregulators: fine-tuning metabolism. Cell Metab. *20*, 26-40.

120. Mounier, C., Bouraoui, L., and Rassart, E. (2014). Lipogenesis in cancer progression. Int J Oncol. *45*(2), 485-492.

121. Nielsen, H., Engelbrecht, J., Brunak, S., and von Heijne, G. (1997). Identification of prokaryotic and eukaryotic signal peptides and prediction of their cleavage sites. Protein Eng. *10*(1), 1-6.

122. Ngo, H. B., Lovely, G. A., Phillips, R., and Chan, D. C. (2014). Distinct structural features of TFAM drive mitochondrial DNA packaging versus transcriptional activation. Nat Commun. *5*, 3077.

123. Nicholls, D.G. (1974). Hamster brown-adipose-tissue mitochondria. The chloride permeability of the inner membrane under respiring conditions, the influence of purine nucleotides. Eur J Biochem. *49*, 585-93.

124. Park, A., Kim, W.K., and Bae, K.H. (2014). Distinction of white, beige and brown adipocytes derived from mesenchymal stem cells. World J Stem Cells. *6*, 33e42.

125. Pearce, S. F., Rebelo-Guiomar, P., D'Souza, A. R., Powell, C. A., Van Haute, L., and Minczuk, M. (2017). Regulation of Mammalian Mitochondrial Gene Expression: Recent Advances. Trends Biochem Sci. *42*(8):625-639.

126. Peirce, V., Carobbio, S., and Vidal-Puig, A. (2014). The different shades of fat. Nature. *510*, 76–83.

127. Peralta, S., Wang, X., and Moraes, C. T. (2012). Mitochondrial transcription: lessons from mouse models. Biochim. Biophys. Acta, Gene Regul. Mech. *1819*(9), 961-969.

128. Perry, R.J., Camporez, J.P.G., Kursawe, R., Titchenell, P.M., Zhang, D., Perry, C.J., Jurczak, M.J., Abudukadier, A., Han, M.S., Zhang, X.M. and Ruan, H.B. (2015). Hepatic acetyl CoA links adipose tissue inflammation to hepatic insulin resistance and type 2 diabetes. Cell. *160*(4), 745-758.

129. Porras, D.P., Abbaszadeh, M., Bhattacharya, D., D'Souza, N.C., Edjiu, N., Perry, C.G.R., and Scimè, A. (2017). p107 determines a metabolic checkpoint required for adipocyte lineage fates. Stem Cells. *35,* 1378-1391.

130. Porstmann, T., Santos, C.R., Griffiths, B., Cully, M., Wu, M., Leevers, S., Griffiths, J.R., Chung, Y.L. and Schulze, A. (2008). SREBP activity is regulated by mTORC1 and contributes to Akt-dependent cell growth. *Cell metab*. *8*(3), 224-236.

131. Puca, A. A., Chatgilialoglu, C., and Ferreri, C. (2008). Lipid metabolism and diet: Possible mechanisms of slow aging. Int. J. Biochem. Cell Biol. *40*(3), 324-333.

132. Rafalski, V.A., Mancini, E., and Brunet, A. (2012). Energy metabolism and energy-sensing pathways in mammalian embryonic and adult stem cell fate. J. Cell. Sci. *125*, 5597-5608.

133. Richon, V. M., Lyle, R. E., and McGehee, R. E. (1997). Regulation and expression of retinoblastoma proteins p107 and p130 during 3T3-L1 adipocyte differentiation. J Biol Chem. *272*, 10117-10124.

134. Roberti, M., Bruni, F., Loguercio Polosa, P., Manzari, C., Gadaleta, M.N., and Cantatore, P. (2006). MTERF3, the most conserved member of the mTERF-family, is a modular factor involved in mitochondrial protein synthesis. Biochem Biophys Acta. *1757*, 1199–1206.

135. Rosell, M., Kaforou, M., Frontini, A., Okolo, A., Chan, Y., Nikolopoulou, E., Millership, S., Fenech, M.E., MacIntyre, D., Turner, J.O., Moore, J.D., Blackburn, E., Gullick, W.J., Cinti, S., Montana, G., Parker, M.G., and Christian, M. (2014). Brown and white adipose tissues:

intrinsic differences in gene expression and response to cold exposure in mice. Am J Physiol Endrocrinol Metab. *306*, E945-64.

136. Rosen, E. D., and MacDougald, O. A. (2006). Adipocyte differentiation from the inside out. *Nature reviews.* Mol Cell Biol, *7*(12), 885.

137. Rosen, E.D and Spiegelman, B.M. (2011). Adipocytes as regulators of energy balance and glucose homeostasis. Nature. *444,* 847-853.

138. Ross, A. S., Tsang, R., Shewmake, K., and McGehee, R. E. (2008). Expression of p107 and p130 during human adipose-derived stem cell adipogenesis. Biochem. Biophys. Res. Commun. *366*(4), 927-931.

139. Rowe, G.C., Patten, I.S., Zsengeller, Z.K., El-Khoury, R., Okutsu, M., Bampoh, S., Koulisis, N., Farrell, C., Hirshman, M.F., Yan, Z. and Goodyear, L.J., (2013). Disconnecting mitochondrial content from respiratory chain capacity in PGC-1-deficient skeletal muscle. Cell Rep. *3*(5), 1449-1456.

140. Safdar, A., Khrapko, K., Flynn, J.M., Saleem, A., Lisio, M., Johnston, A.P., Kratysberg, Y., Samjoo, I.A., Kitaoka, Y., Ogborn, D.I. and Little, J.P. (2016). Exercise-induced mitochondrial p53 repairs mtDNA mutations in mutator mice. Skelet muscle, *6*(1), 7.

141. Sanchez-Gurmaches, J., Hung, C.M., and Guertin, D.A. (2016). Emerging complexities in adipocyte origins and identity. Trends Cell Biol. *26*, 31326.

142. Sancho, P., Barneda, D., and Heeschen, C. (2016). Hallmarks of cancer stem cell metabolism. Br. J. Cancer. *114*(12), 1305.

143. Saponaro, C., Gaggini, M., Carli, F., and Gastaldelli, A. (2015). The subtle balance between lipolysis and lipogenesis: a critical point in metabolic homeostasis. Nutrients, *7*(11), 9453-9474.

144. Schon, E.A., DiMauro, S., and Hirano, M. (2012). Human mitochondrial DNA: roles of inherited and somatic mutations. Nat Rev Genet. *13*, 878-890.

145. Scuteri, A., Sanna, S., Chen, W.M., Uda, M., Albai, G., Strait, J., Najjar, S., Nagaraja, R., Orrú, M., Usala, G. and Dei, M., 2007). Genome-wide association scan shows genetic variants in the FTO gene are associated with obesity-related traits. PLoS Genet. *3*(7), e115.

146. Seale, P., Bjork, B., Yang, W., Kajimura, S., Kuang, S., Scime, A., Devarakonda, S., Chin, S., Conroe, H.M., Erdjument-Bromage, H. and Tempst, P. (2008). PRDM16 controls a brown fat/skeletal muscle switch. Nature. *454*(7207), 961.

147. Seale, P., Kajimura, S., and Spiegelman, B.M. (2009). Transcriptional control of brown adipocyte development and physiological function of mice and men. Genes & Dev. *23*, 788e97.

148. Sellers, W.R, Rodgers, J.W., and Kaelin, W.G. Jr. (1995). A potent transrepression domain in the retinoblastoma protein induces a cell cycle arrest when bound to E2F sites. Proc Natl Acad Sci. *92*, 11544-11548.

149. Shao, W., Yu, Z., Chiang, Y., Yang, Y., Chai, T., Foltz, W., Lu, H., Fantus, I.G. and Jin, T. (2012). Curcumin prevents high fat diet induced insulin resistance and obesity via attenuating lipogenesis in liver and inflammatory pathway in adipocytes. *PloS one*, *7*(1), e28784.

150. Shore, A.M., Karamitri, A., Kemp, P., Speakman, J.R., Graham, N.S., and Lomax, M.A. (2013). Cold-induced changes in gene expression in brown adipose tissue, white adipose tissue and liver. PlOS ONE. *8*, e68933.

151. Shyh-Chang, N., Daley, G.Q., Lewis, C., and Cantley, L.C. (2013). Stem cell metabolism in tissue development and aging. Development. *140*, 2535-2547.

152. Sidossia, L. and Kajimura, S. (2015). Brown and beige fat in humans: thermogenic adipocytes that control energy and glucose homeostasis. J Clin Invest. *125*, 478-486.

153. Solinas, G., Borén, J., and Dulloo, A. G. (2015). De novo lipogenesis in metabolic homeostasis: More friend than foe? Mol Metab. *4*(5), 367-377.

154. Spangenberg, L., Shigunov, P., Abud, A.P.R., Cofre, A.R., Stimamiglio, M.A., Kuligovski, C., Zych, J., Schittini, A.V., Costa, A.D.T., Rebelatto, C.K., Brofman, P.R.S., Goldenberg, S., Correa, A., Naya, H., and Dallagiovanna, B. (2013). Polysome profiling shows extensive posttranscriptional regulation during human adipocyte stem cell differentiation into adipocytes. Stem Cell Res. *11*, 902-912.

155. Strålfors, P., and Belfrage, P. (1983). Phosphorylation of hormone-sensitive lipase by cyclic AMP-dependent protein kinase. J Biol Chem. *258*(24), 15146-15152.

156. Susulic, Vedrana S., Robert C. Frederich, Joel Lawitts, Effie Tozzo, Barbara B. Kahn, Mary-Ellen Harper, Jean Himms-Hagen, Jeffrey S. Flier, and Bradford B. Lowell. (1995). Targeted disruption of the β3-adrenergic receptor gene. J Biol Chem. *270*(49), 29483-29492.

157. Takeuchi, Y., Yahagi, N., Aita, Y., Murayama, Y., Sawada, Y., Piao, X., ... and Masuda, Y. (2016). KLF15 enables rapid switching between lipogenesis and gluconeogenesis during fasting. Cell Rep. *16*(9), 2373-2386.

158. Takeuchi, Y., Yahagi, N., Aita, Y., Murayama, Y., Sawada, Y., Piao, X., Toya, N., Oya, Y., Shikama, A., Takarada, A. and Masuda, Y. (2004). Commitment of C3H10T1/2 pluripotent stem cells to the adipocyte lineage. Proc. Natl. Acad. Sci. U.S.A. *101*(26), 9607-9611.

159. Tchkonia, T., Thomou, T., Zhu, Y., Karagiannides, I., Pothoulakis, C., Jensen, M.D., and Kirkland, J.L. (2013). Mechanisms and metabolic implications of regional differences among fat depots. Cell Metab. *17*, 644–56.

160. Townsend, K. L., and Tseng, Y. H. (2014). Brown fat fuel utilization and thermogenesis. Trends Endocrinol Metab. *25*(4), 168-177.

161. Turner, N., and Heilbronn, L. K. (2008). Is mitochondrial dysfunction a cause of insulin resistance?. Trends Endocrinol Metab. *19*(9), 324-330.

162. Umekawa, T., Yoshida, T., Sakane, N., Saito, M., Kumamoto, K., and Kondo, M. (1997). Anti-obesity and anti-diabetic effects of CL316,243, a highly specific beta 3-adrenoceptor agonist, in Otsuka Long-Evans Tokushima Fatty rats: induction of uncoupling protein and activation of glucose transporter 4 in white fat. Eur. J.Endocrinol. *136*, 429-437.

163. Unami, A., Shinohara, Y., Kajimoto, K., and Baba, Y. (2004). Comparison of gene expression profiles between white and brown adipose tissues of rat by microarray analysis. Biochem Pharmacol. *67*, 555–564.

164. Vaillancourt, E., Haman, F., & Weber, J. M. (2009). Fuel selection in Wistar rats exposed to cold: shivering thermogenesis diverts fatty acids from re-esterification to oxidation. J Physiol. 587, 4349-59.

165. Van der Knaap, J.A. and Verrijzer, C.P. (2016). Undercover: gene control by metabolites and metabolic enzymes. Genes & Dev. *30*, 2345-2369.

166. Vazquez-Vela, M.E.F., Torres, N., Tovar, A.R., (2008). White Adipose Tissue as Endocrine Organ and Its Role in Obesity. Elsevier. *39*, 715-728.

167. Ventura-Clapier, R., Garnier, A., and Veksler, V. (2008). Transcriptional control of mitochondrial biogenesis: the central role of PGC-1α. Cardiovasc Res. *79*, 208-217.

168. Vitali, A., Murano, I., Zingaretti, M.C., Frontini, A., Ricquier, D., and Cinti, S. (2012). The adipose organ of obesity-prone C57BL/6J mice is composed of mixed white and brown adipocytes. J Lipid Res. *53*, 619–629.

169. Walden, T.B., Hansen, I.R., Timmons, J.A., Cannon, B., and Nedergaard, J. (2012). Recruited vs. nonrecruited molecular signatures of brown, ‘‘brite,’’ and white adipose tissues. Am J Physiol Endocrinol Metab. *302*, E19–31.

170. Wang, Q., Li, Y. C., Wang, J., Kong, J., Qi, Y., Quigg, R. J., and Li, X. (2008). miR-17-92 cluster accelerates adipocyte differentiation by negatively regulating tumor-suppressor Rb2/p130. Proc. Natl. Acad. Sci. U.S.A. *105*(8), 2889-2894.

171. Wang, Q.A., Tao, C., Gupta, R.K., and Scherer, P.E. (2013). Tracking adipogenesis during white adipose tissue development, expansion and regeneration. Nat. Med. *19*, 1338-1344.

172. Watanabe, M., Yamamoto, T., Kakuhata, R., Okada, N., Kajimoto, K., Yamazaki, N., Kataoka, M., Baba, Y., Tamaki, T., and Shinohara, Y. (2008b). Synchronized changes in transcript levels of genes activating cold exposure-induced thermogenesis in brown adipose tissue of experimental animals. Biochem Biophys Acta. 1777, 104–112.

173. Watanabe, M., Yamamoto, T., Mori, C., Okada, N., Yamazaki, N., Kajimoto, K., Kataoka, M., and Shinohara, Y. (2008a). Cold-induced changes in gene expression in brown adipose tissue: implications for the activation of thermogenesis. Biol Pharm Bull. 31, 775–784.

174. Watanabe, M., Yamamoto, T., Yamamoto, A., Obana, E., Niiyama, K., Hada, T., Ooie, T., Kataoka, M., Hori, T., Houchi, H., and Shinohara, Y. (2011). Differential effects of cold exposure on gene expression profiles in white versus brown adipose tissue. Appl Biochem Biotechnol. *165*, 538–547.

175. Wijkander, J., Landström, T. R., Manganiello, V., Belfrage, P., and Degerman, E. (1998). Insulin-induced phosphorylation and activation of phosphodiesterase 3B in rat adipocytes: possible role for protein kinase B but not mitogen-activated protein kinase or p70 S6 kinase. J Endocrinol. *139*(1), 219-227.

176. Wu, J., Bostrom, P., Sparks, L.M., Ye, L., Choi, J.H., Giang, A., Khandekar, M., Virtanen, K.A., Nuutila, P., Schaart, G., Huang, K., Tu, H., van Marken Lichtenbelt, W.D., Hoeks J., Enerback, S., Schrauwen, P., and Spiegelman, B.M. (2012). Beige adipocytes are a distinct type of thermogenic fat cell in mouse and human. Cell. *150*, 366–376.

177. Wu, Z., Puigserver, P., Andersson, U., Zhang, C., Adelmant, G., Mootha, V., Troy, A., Cinti, S., Lowell, B., Scarpulla, R.C. and Spiegelman, B.M. (1999). Mechanisms controlling mitochondrial biogenesis and respiration through the thermogenic coactivator PGC-1. Cell. *98*, 115–124.

178. X'avia, C. Y., Black, C. M., Lin, A. J., Ping, P., and Lau, E. (2015). Mitochondrial protein turnover: methods to measure turnover rates on a large scale. J. Mol. Cell. Cardiol. *78*, 54-61.

179. Yakubovskaya, E., Mejia, E., Byrnes, J., Hambardjieva, E., and Garcia-Diaz, M. (2010). Helix unwinding and base flipping enable human MTERF1 to terminate mitochondrial transcription. Cell Metab. *141*, 982–993.

180. Yamamoto, T., Yamamoto, A., Watanabe, M., Kataoka, M., Terada, H., and Shinohara, Y. (2011). Quantitative evaluation of the effects of cold exposure of rats on the expression levels of ten FABP isoforms in brown adipose tissue. Biotechnol Lett. *33*, 237–242.

181. Yamazaki, N., Shinohara, Y., Shima, A., and Terada, H. (1995). High expression of a novel carnitine palmitoyltransferase I like protein in rat brown adipose tissue and heart: isolation and characterization of its cDNA clone. FEBS Lett. *363*, 41–45.

182. Yang, K.J., Noh, J-R., Kim, Y-H., Gang, G-T., Hwang, J-H., Yang, S.J., Yeom, Y.I., and Lee, C.H. (2010). Differential modulatory effects of rosiglitazone and pioglitazone on white adipose tissue in db/db mice. Life Sciences. *87*, 405-410.

183. Zhang, J., Khvorostov, I., Hong, J.S., Oktay, Y., Vergnes, L., Nuebel, E., Wahjudi, P.N., Setoguchi, K., Wang, G., Do, A., Jung, H.J., McCaffery, J.M., Kurland, I.J., Reue, K., Lee, W.N., Koehler, C.M., and Teitell, M.A. (2011). UCP2 regulates energy metabolism and differentiation potential of human pluripotent stem cells. EMBO J. *30*, 4860-73.

184. Zhou, W., Choi, M., Margineantu, D., Margaretha, L., Hesson, J., Cavanaugh, C., Blau, C.A., Horwitz, M.S., Hockenbery, D., Ware, C., and Ruohola-Baker, H. (2012). HIF1α induced switch from bivalent to exclusively glycolytic metabolism during ESC-to-EpiSC/hESC transition. EMBO J. *31*, 2103-16.